

Loss of Topoisomerase I leads to R-loop-mediated transcriptional blocks during ribosomal RNA synthesis

Aziz El Hage, Sarah L. French¹, Ann L.Beyer¹ and David Tollervey²

Wellcome Trust Centre for Cell Biology,
University of Edinburgh,
Edinburgh EH9 3JR,
UK

1 Department of Microbiology,
University of Virginia Health System,
Charlottesville, VA 22908-0734
USA

2 Corresponding author:
E-mail: d.tollervey@ed.ac.uk
Tel: (44) 131 650 7092
Fax: (44) 131 650 7040

Keywords: rRNA synthesis, RNA polymerase I, transcription elongation, topoisomerase, rDNA, RNase H, R-loops, RNA/DNA hybrids, transcription pausing

Running title: Pol I transcription and R-loops

62,646 characters (with spaces)

ABSTRACT

Pre-rRNA transcription by RNA Polymerase I (Pol I) is very robust on active rDNA repeats. Loss of yeast topoisomerase I (Top1) generated truncated pre-rRNA fragments, which were stabilized in strains lacking TRAMP or exosome degradation activities. Loss of both Top1 and Top2 blocked pre-rRNA synthesis, with pre-rRNAs predominately truncated in the 18S 5' region. Positive supercoils in front of Pol I are predicted to slow elongation, while rDNA opening in its wake might cause R-loop formation. CHIP analysis showed substantial levels of RNA/DNA hybrids in the wild-type, particularly over the 18S 5' region. The absence of RNase H1 and H2 in cells depleted of Top1 increased the accumulation of RNA/DNA hybrids and reduced pre-rRNA truncation and pre-rRNA synthesis. Hybrid accumulation over the rDNA was greatly exacerbated when Top1, Top2 and RNase H were all absent. EM analysis revealed Pol I pile-ups in the wild-type, particularly over the 18S. Pile-ups were longer and more frequent in the absence of Top1 and their frequency was exacerbated when RNase H activity was also lacking. We conclude that the loss of Top1 enhances inherent R-loop formation, particularly over the 5' region of the rDNA, imposing persistent transcription blocks when RNase H is limiting.

INTRODUCTION

Yeast rDNA is comprised of ~150-200 tandem repeats, about half of which are actively transcribed. The primary transcript of 35S pre-rRNA is processed into the mature 18S rRNA component of the 40S ribosome subunit and 5.8S and 25S rRNA components of the 60S subunit (see Figs. 1A and S1). Active rDNA repeats are heavily transcribed by RNA Pol I, as visualized by “Miller” chromatin spreads (French et al. 2003), and this was proposed to involve “transcription factories” where the DNA template is reeled through a polymerase array with constrained mobility (reviewed in (Cook 1999; Sutherland and Bickmore 2009)).

EM analyses (Osheim et al. 2004) and metabolic labeling (Kos and Tollervey 2010) demonstrate that ~50-70% of yeast pre-rRNA transcripts are cleaved cotranscriptionally. This indicates that yeast pre-ribosome assembly is at least partly cotranscriptional. Consistent with this, ribosome assembly is impaired in mutants with defects in Pol I elongation, indicating a coupling between these processes (Schneider et al. 2007; Zhang et al. 2009). Surveillance systems monitor yeast ribosome synthesis and the pre-rRNA components of aberrant pre-ribosomes are polyadenylated by the Trf4/Trf5–Air1/Air2-Mtr4 polyadenylation complexes (TRAMP) and targeted for degradation by the exosome nuclease complex (Dez et al. 2006; Schneider et al. 2007; Wery et al. 2009).

During transcription either the DNA or the polymerase must rotate once for every ~10nt transcribed. DNA rotation generates positive supercoils (more tightly wound DNA) ahead of the transcription bubble, whereas negative supercoils (more loosely wound DNA) are left behind the polymerase (reviewed by (Wang and Lynch 1993; Cook 1999)). Eukaryotic Topoisomerases I (Top1) and II (Top2) are able to relax both positive and negative DNA supercoils (reviewed in (Wang 2002)) and play essential roles during rDNA transcription in *S.cerevisiae* (Brill et al. 1987; Schultz et al. 1992).

The accumulation of positive supercoiling ahead of the transcription bubble resists opening of the DNA, which can slow or impede transcription elongation by Pol I (Zhang et al. 1988), as seen following treatment with the Top1 inhibitor camptothecin (Koster et al. 2007). In contrast, negative supercoiling behind the transcription bubble can lead to opening of the DNA. When this happens, the nascent RNA may hybridize to the transcribed strand creating RNA-DNA hybrids known as R-loops (Drolet 2006). R-loops can also impede transcription elongation, as well as exposing the non-template strand to cleavage and recombination (reviewed in (Aguilera and Gomez-Gonzalez 2008)). Yeast *top1Δ* mutants show hyper-recombination of the rDNA array (Houseley et al. 2007), while *top1Δ top2-ts* double mutants undergo major excisions of the rDNA repeats due to a failure to relax negative supercoils (Trigueros and Roca 2002).

R-loops can be removed by cleavage by RNase H1 and RNase H2, which have overlapping functions and similar catalytic mechanisms (Arudchandran et al. 2000). Yeast RNase H1 is a single protein, whereas RNase H2 is a complex of three proteins, Rnh2A (Rnh201), Ydr279 (Rnh202) and Ylr154 (Rnh203) (Jeong et al. 2004). 70% of RNase H activity is lost upon deletion of *RNH201* (Jeong et al. 2004). However, *rnh1Δ rnh201Δ* double mutant strains are viable, indicating that they retain some RNase H activity. Moreover, a residual activity was still able to degrade poly(rA):poly(dT) substrates in double mutant cell extract (Arudchandran et al. 2000), confirming that an additional RNase H activity exists. Yeast RNase H is reported to alleviate transcriptional blocks in THO-complex mutants (Huertas and Aguilera 2003), and to destroy RNA-DNA hybrids formed by telomeric TERRA transcripts that accumulate in the absence of Rat1 5'-3' exonuclease activity (Luke et al. 2008). In higher Eukaryotes, over-expression of RNase H can suppress the genomic instability otherwise induced by R-loop formation following depletion of the pre-mRNA splicing factor ASF/SF2 (Li and Manley 2005) or Topoisomerase 1 (Tuduri et al. 2009).

TOP1 deletion was reported to be synthetic lethal with deletion of the genes encoding the RNA Pol I subunits Rpa34/Rpa49 (Beckouet et al. 2008) a heterodimer that functions during Pol I transcription initiation and elongation (Kuhn et al. 2007; Beckouet et al. 2008). The Trf4 component of the TRAMP complex also interacts genetically with Top1, suggesting further links between pre-rRNA metabolism and rDNA structure (Houseley et al. 2007).

Here we show that Pol I transcription in the absence of Top1 is facilitated by RNase H activity, via cleavage of RNA-DNA hybrids engaged in R-loops. We also report that the 5' end of the 18S rDNA poses problems during pre-rRNA transcription even in the wild-type, which are exacerbated when both Top1 and Top2 are absent, and represents the major site for R-loop formation.

RESULTS

Aberrant pre-rRNA fragments are generated in top1Δ mutants and targeted for degradation by the exosome and TRAMP complexes

To investigate the effects of loss of Top1 on rRNA synthesis, total RNA extracted from WT and *top1Δ* strains was analyzed by Northern. Several truncated species were identified (labeled 1–9 in Fig. 1), which were mapped by comparison of hybridization patterns using multiple probes across the 35S pre-rRNA (see Fig. 1A).

Two major truncated pre-rRNAs, species 3 and 4 were detected with probes 130 and 033, which hybridize to different regions of the 5'-ETS (Figs. 1B lane 3 and 1F lanes 2 and 7) but not with probe 004, which hybridizes between sites D and A2 (Fig. 1C lane 3). The RNAs were separated on agarose gels, which have limited resolution, but species 3 and 4 have estimated size of ~ 1.1 Kb and ~2.1 Kb, respectively. This indicates that species 3 extends from the 5' end of the pre-rRNA to a position ~0.4 Kb into the 18S rRNA region, while species 4 extends ~1.4 Kb into 18S. Two less abundant RNAs, species 5 (~4 Kb) and 6 (~6 Kb), are predicted to extend from the 5' end of the pre-rRNA to sites within the 25S rRNA (Fig. 1F lanes 2 and 7). Species 7 and 8 have 5' ends at the cotranscriptional cleavage site A2, since they were detected with probe 003 (which lies 3' to site A2), but not with 004 (5' to A2) (Figs. 1D lane 3, 1G lane 1 and S3B, lane 2). Species 7 was ~0.4 - 0.5 Kb in size, corresponding to 3' ends within ITS2, whereas species 8 was ~1.2 Kb, corresponding to a 3' end ~ 0.4 Kb into the 25S rRNA region.

The presence of these truncated pre-rRNA species strongly suggested that the absence of Top1 impedes Pol I transcription, leading to cleavage or release of nascent pre-rRNAs.

In other mutants, aberrant pre-ribosomes are targeted cotranscriptionally by the TRAMP nuclear surveillance complex and degraded by the exosome (Dez et al. 2006; Schneider et al. 2007; Wery et al. 2009). We therefore deleted the gene encoding the non-essential, nuclear exosome component Rrp6 in *top1Δ* strains. The *top1Δ rrp6Δ* double mutant strain showed strongly increased accumulation of RNA species 3, 4 (Figs. 1B lane 4 and 1F lane 4), 7 and 8 (Figs. 1D lane 4 and S3B, lane 4) relative to the *top1Δ* single mutant. Additional pre-rRNA species were also detected; probe 130, which lies close to the 5' end of the pre-rRNA primary transcript, detected a small RNA of ~240 nt designated species 1 (Fig. 1F lane 4 and S3A, lane 4), while 5'-ETS probes 130 and 033 detected an RNA with a size below 1 Kb designated species 2 (Figs. 1B lane 4 and 1F lane 4).

Surveillance of aberrant pre-rRNAs by the TRAMP complex is associated with RNA polyadenylation. Purification of poly(A)⁺ RNAs from the *top1Δ rrp6Δ* strain showed that species 2, 3, 4 (Fig. 1B lane 8) and 8 (Fig. 1D lane 8) are indeed polyadenylated. In contrast, species 7

was not detectably polyadenylated (Fig. 1D lane 8), although it remains possible that short oligo(A) tails were present and escaped our purification method. Deletion of *TRF4* in a *top1Δ* background led to stabilization of species 1, 2 (probe 130, Figs. 1F lane 8 and 1G upper panel lane 2), and 7 and 8 (probe 003, Fig. 1G lane 2).

Pre-rRNA fragments extending from the 5' end of the rDNA into the 5' region of the 18S were detected with probes 130 and 033 in both single *rrp6Δ* and double *trf4Δ rrp6Δ* mutants (*TOP1⁺*) (species labeled 2-3, Fig. 1F lanes 3 and 6). Thus, Pol I transcription through the 5' region of the 18S rDNA might be a limiting step even in otherwise wild-type cells, as previously proposed (Schneider et al. 2007).

In conclusion, the absence of Top1 leads to the accumulation of two major groups of RNAs; species 1 to 4 extend from the transcription start site to sites within the 5'-ETS and 18S rDNA, whereas species 7 and 8 extend from the A2 site of cotranscriptional cleavage to positions in ITS2 and the 5' region of the 25S rDNA (see Fig. 1A). These aberrant pre-rRNAs are polyadenylated by TRAMP and degraded by the exosome.

Pre-rRNA fragments are increased in top1Δ mutants at low growth temperatures

If positive supercoiling before, and/or negative supercoiling behind transcribing Pol I restrict elongation in *top1Δ* strains, this might be exacerbated by a more rigid DNA structure at lower growth temperatures (Drolet 2006). To assess this, *top1Δ* strains were grown at 18, 25 or 30°C. Northern analyses showed that accumulation of truncated RNA species 3 to 6 (probe 130, Fig. 2A) and 7 to 9 (probe 003, Figs. 2B-C) progressively increased from 30°C to 25°C to 18°C. The ratio between species 3 and 4 increased as growth temperature decreased (Fig. 2A compare lanes 6, 4 and 2). Comparison of the levels of truncated pre-rRNA species with those of 35S pre-rRNA (Figs. 2A-C) showed that species 3 and 4 are more abundant than species 7, 8 and 9, arguing against the possibility that all these fragments might be generated by cleavage of a single truncated pre-rRNA species.

At 18°C, synthesis of 27S pre-rRNA was reduced, whereas levels of 20S pre-rRNA were little affected (Figs. 2D-E, probes 004 and 003) (see Fig. S1 for the rRNA maturation pathway). Fast tritium-labeling experiments performed according to Kos and Tollervey (2010) at 25°C showed that the kinetics of co- and post- transcriptional processing of pre-rRNA species 35S, 20S and 27S are delayed in the *top1Δ* mutant relative to the wild-type (data not shown). At lower temperatures, increased transcriptional blockages in particular in the 5' region of 18S would affect the synthesis of all pre-rRNA species. However blockages downstream of site A2 (Fig. S1)

would affect only 27S and 35S synthesis, potentially leading to the observed increase in 20S to 27S ratios.

These data indicate that rRNA synthesis in *top1Δ* strains is more affected at low growth temperatures, where excess supercoils may be more frequent and/or stable (Baaklini et al. 2008). The predominance of species 3 at lower temperatures suggests increased transcription blockage in the 5' region of 18S rDNA, with reduced synthesis of downstream RNA species. Increased transcription elongation defects may also produce the elevated 20S to 27S pre-rRNA ratio seen at low temperatures.

rRNA transcription stalls in the 5' region of the 18S rDNA in the absence of both Top1 and Top2

Although pre-rRNAs were truncated and degraded in the absence of Top1, synthesis of full-length pre-rRNA was only partially inhibited. Top1 is partially redundant with Top2 and rRNA synthesis is fully inhibited in double *top1Δ top2-ts* strains at non-permissive temperature (Brill et al. 1987; Schultz et al. 1992). To analyze rRNA synthesis and pre-rRNA fragment accumulation in the absence of Top2 or both Top1 and Top2, we constructed single *P_{GAL}-TOP2* and double *P_{GAL}-TOP2 top1Δ* strains. As expected, both mutant strains showed growth inhibition in glucose medium, since Top2 is essential for viability in yeast. Northern analyses detected no major rRNA synthesis defects in the single *P_{GAL}-TOP2* strain even after several hours of depletion (Figs. 3B-H lanes 1-6 and S3A-F lanes 9-14). In double *P_{GAL}-TOP2 top1Δ* strains, depletion of Top2 reduced formation of truncated species 4 relative to the *top1Δ* single mutant (Fig. 3B, compare lane 7 with 8-11). Formation of the normal 35S, 20S, 27S (Figs. 3B-D, lanes 7-11) and 7S (Fig. S3C, lanes 15-19) pre-rRNAs was also inhibited. However, this was not the case for truncated species 1 and 3 (Figs. 3B, lanes 7-11 and S3A, lanes 15-19). In addition, multiple heterogeneous species were detected in the double mutant, with predicted 3' ends at sites encompassing the region from site A₀ (+600 nt in 5'-ETS) to ~500 nt into the 18S rDNA region (Figs. 3A, 3B and S3A, species labeled by stars).

The accumulation of these truncated fragments, together with the loss of fragment 4 (see Fig. 3A) and all normal pre-rRNAs, strongly indicates that Pol I elongation is predominately arrested within the 5' region of the 18S rDNA in strains lacking both Top1 and Top2.

Northern analyses on RNA from a *top1Δ top2-ts* strain gave similar results, showing the preferential loss of truncated species 4 relative to 1 and 3 at the restrictive temperature of 37°C (Fig. S4A lanes 1-2) as well as significant reductions in the 20S and 27S pre-rRNAs.

Together the data indicate that in the absence of Top1 alone Pol I transcription elongation is mainly affected over the 18S sequences. In the absence of Top1 at lower growth temperatures, or when Top1 is lacking and Top2 limiting, transcriptional blocks become predominant in the 5' region of 18S, leading to the inhibition of rRNA synthesis.

The absence of both Top1 and RNase H inhibits rRNA synthesis and increases ncRNA expression from IGS spacers

If the absence of Top1, or both Top1 and Top2, results in rDNA opening behind Pol I, the associated, nascent pre-rRNA transcripts may form R-loops with the DNA template. R-loops are predicted targets for RNase H activity, which might therefore generate the observed pre-rRNA fragments.

A recent analysis reported that over-expression of the Rnh201 subunit of RNase H2 increased degradation of RNA-DNA hybrids over telomeric regions in the 5'-3' exonuclease *rat1-1* mutant (Luke et al. 2008). However, over-expression of Rnh201 in a *top1Δ* mutant did not alter the abundance or distribution of pre-rRNA fragments (Figs. S2). This was also the case for over-expression of Rnh1 or Rnh201 in *top1Δ top2-ts* mutant at 25°C and 37°C (Fig. S4).

To test whether pre-rRNA fragments accumulated in *top1Δ* mutants are generated by RNase H cleavage, we initially attempted to delete both *RNH1* and *RNH201* in *top1Δ* strains. Deletion of both *RNH1* and *RNH201* in *TOP1* strains had no detectable effect on growth (data not shown and (Arudchandran et al. 2000)), or rRNA synthesis (Figs. 4B-H, compare lanes 1 and 9). However, we could not delete both *RNH1* and *RNH201* in *top1Δ* strains suggesting that *top1Δ*, *rnh1Δ* and *rnh201Δ* are lethal in combination. We therefore placed *TOP1* expression under the control of a conditional P_{GAL} promoter and deleted both *RNH1* and *RNH201* in this strain. Northern analyses were performed using total RNA extracted from single P_{GAL} -*TOP1* and triple P_{GAL} -*TOP1 rnh1Δ rnh201Δ* mutants, which were shifted from permissive galactose (0 hr) to non-permissive glucose containing medium for 2 to 14 hr at 30°C.

Growth of the single P_{GAL} -*TOP1* mutant strain was only slightly inhibited after shift to glucose, consistent with the viability of *top1Δ* mutants (data not shown). Growth of the P_{GAL} -*TOP1 rnh1Δ rnh201Δ* triple mutant strain slowed after 10 hr of Top1 depletion in glucose-containing medium, and completely ceased after ~14 to 16 hr (data not shown).

Northern hybridization showed a marked reduction in accumulation of truncated pre-rRNA fragments 3, 4, 8 and 9 in the triple mutant relative to the single mutant during Top1 depletion (Figs. 4B-C). Accumulation of 27S but not 20S was decreased in the single mutant during Top1 depletion (Figs. 4D-E, lanes 1-8 and Figs. 4I-J) as was observed in *top1Δ* strains

(see Figs. 2D-E). In contrast, both 20S and 27S accumulation decreased in the triple mutant (Figs. 4D-E, lanes 9-16 and Figs. 4I-J).

At early times of Top1 depletion (6 hr) the triple-mutant showed reductions in both pre-rRNA truncation and synthesis of 20S and 27S pre-rRNA (Figs. 4B-D, lane 12). In the absence of both Top1 and RNase H1 and H201, stable RNA-DNA hybrids may impose transcriptional blocks along the rDNA further reducing pre-rRNA transcription, as shown *in vitro* (Tous and Aguilera 2007). This is supported by the almost complete disappearance of pre-rRNA fragments in the triple mutant after 14 hours of Top1 depletion (Figs. 4B-C lane 16). The reduced level of pre-rRNA fragments still seen in the triple $P_{GAL}\text{-TOP1 } mh1\Delta mh201\Delta$ mutant after 6 hr of Top1 depletion could arise from the residual RNase H activity previously observed in extracts from strains lacking both RNase H1 and H201 (Arudchandran et al. 2000) or from other RNA cleavage activities (see Discussion).

RNA Pol II generates non protein-coding RNA transcripts (ncRNA) from the rDNA intergenic spacers (IGS1 and IGS2). Northern hybridization showed that ncRNAs IGS1-F and IGS2-R accumulated in mutants lacking Top1 (Figs. 3E lane 7 and 4G lanes 7-8), as previously reported (Houseley et al. 2007). Accumulation of these transcripts increased strongly in the triple mutant (Fig. 4G lanes 9-16), but this was not the case in the $P_{GAL}\text{-TOP2 } top1\Delta$ strain depleted of Top2 (Fig. 3E lanes 7-11). Transcription of IGS1-F and IGS2-R is normally limited by a repressive chromatin structure that requires the histone deacetylase Sir2 (Li et al. 2006). IGS transcription in mutants lacking Top1 is possibly due to disruption of the chromatin structure caused by accumulation of supercoils in IGS1 and IGS2 regions. The increase in ncRNA levels seen in the triple mutant strain indicates a specific role for RNase H in the synthesis or degradation of IGS transcripts.

RNA-DNA hybrids accumulate over the Pol I promoter, the 5'-ETS and the IGS regions of the rDNA when both Top1 and RNase H are absent

The accumulation of pre-rRNA fragments with 3' ends within the 5' region of the 18S rRNA, in the absence of Top1 alone or both Top1 and Top2, strongly suggested that Pol I might have to overcome a particular problem that requires topoisomerase activity during transcription of that region.

To gain more insight into the roles of topoisomerase and RNase H activities during Pol I transcription elongation we analyzed by ChIP the distribution of both Pol I (Rpa190) and RNA/DNA hybrids along the rDNA in mutants depleted of Top1, or Top1 and Top2, in the presence or absence of RNase H1 and H201 (Fig. 5). Wild-type (WT), $P_{GAL}\text{-TOP1}$ and $P_{GAL}\text{-}$

TOP1 rnh1Δ rnh201Δ strains were harvested after 6 hr of Top1 depletion in glucose medium at 30°C, at which time growth was little affected in the triple mutant (data not shown). In the WT (Fig. 5A, blue), Pol I (Rpa190) signal was maximal over the 5'-ETS (probe **c**), dropped across the 18S and declined to background levels over the terminator region (probe **m**). ChIP with antibodies directed against the smallest subunit of Pol I (Rpa34-13MYC) gave similar profiles (data not shown). In the single and triple mutants (Fig. 5A, red and green), Pol I signal over the 5'-ETS was shifted towards the promoter region (probes **a-b**) and the overall Pol I signal was decreased in the single and more in the triple mutant.

Together these data suggest that Pol I occupancy is highest over the 5' region of the rDNA. We propose that R-loops and accumulation of positive supercoils in the 5' region of the 18S rDNA slow transcription elongation. Stalling or pausing of any polymerase results in other polymerases becoming backed-up over the upstream regions, and this is particularly frequent in the absence of Top1.

To assess the occurrence of R-loops along the rDNA, we performed ChIP using the S9.6 antibody, which specifically recognizes RNA-DNA hybrids (Boguslawski et al. 1986; Hu et al. 2006) (see Fig. S5 for specificity controls). In the WT (Fig. 5B, blue), RNA-DNA hybrids were detected all along the rDNA, but peaked in the 5' region of 18S (probe **d**, ~0.3 Kb into the 18S rRNA coding region), dropped over the rest of 18S and ITS (probes **e-g**), increased over the 25S and declined over the terminator region (probe **m**). In *rnh1Δ rnh201Δ* (*TOP1+*) cells the RNA-DNA hybrid profile was similar to the WT (data not shown), suggesting that RNA/DNA hybrids detected in the WT are transient.

Profiles of Pol I and RNA/DNA hybrids over the rDNA in the WT do not completely overlap (Figs. 5A and B, blue). We propose that the profile of RNA/DNA hybrids largely reflects the cotranscriptional ribosome assembly pathway (Fig. 5B blue and Fig. 5C). Short nascent pre-rRNA transcripts located towards the 5' end of the gene may be less amenable to R-looping than longer transcripts located further downstream, in particular over the 5' region of 18S. The drop in R-loop occupancy over the second half of 18S and ITS spacers is consistent with the packaging of transcripts to form large "terminal balls" (Osheim et al. 2009; Wery et al. 2009). RNA-DNA hybrids were substantially increased over the Pol I promoter and 5'-ETS sequences in the triple mutant after 6 hr of Top1 depletion (Fig. 5B, green, probes **a-c**). This was not the case in the single mutant, which showed a profile similar to the WT (Fig. 5B, red and blue), suggesting that RNase H1 and H2 are responsible for the cleavage of these RNA/DNA hybrids in the absence of Top1.

RNA-DNA hybrids also increased over the IGS region in the triple mutant (Fig. 5B green, probes **n-p**). This is consistent with the accumulation of Pol II ncRNAs from the rDNA intergenic spacers in the absence of Top1 and RNase H (Fig. 4G, lanes 9-16). The simplest hypothesis would be that cleavage of these RNA-DNA hybrids by RNase H1 and H2 normally limits accumulation of the ncRNAs.

To analyze the distributions of Pol I and RNA/DNA hybrids in the absence of both topoisomerases Top1 and Top2, we placed *TOP2* expression under P_{GAL} promoter in P_{GAL} -*TOP1* and P_{GAL} -*TOP1 rnh1Δ rnh201Δ* strains. WT, P_{GAL} -*TOP1 P_{GAL}-TOP2* (double mutant) and P_{GAL} -*TOP1 P_{GAL}-TOP2 rnh1Δ rnh201Δ* (quadruple mutant) strains were shifted from galactose to glucose medium for 6 hr at 30°C and processed for ChIP analyses. Growth rates decreased in both mutants beginning 4-5 hr post-shift due to depletion of Top1 and Top2 (data not shown). Pol I ChIP signals in the double and quadruple mutants dropped sharply from the 18S centre (Fig. 5D red and green, probe **e**). This sharp decrease in Pol I signal over the 18S and downstream regions is consistent with the conclusion from rRNA analyses (Fig. 3). Transcription elongation in the absence of both Top1 and Top2 is largely blocked in the 5' region of 18S, possibly due to high levels of positive supercoils in this region.

Elevated levels of RNA/DNA hybrids were observed in the *top1 top2* double mutant (Fig. 5E red), but this increase was much more dramatic in the quadruple mutant also lacking RNase H1 and H2 activity, particularly over the 5' region (Fig. 5E green). We postulate that the accumulation of negative supercoils in the absence of both Top1 and Top2 provokes DNA strand separation and the formation of RNA/DNA hybrids, which cannot readily be cleared when RNase H is also deficient. Persistent R-loops are predicted to slow Pol I transcription elongation (Tous and Aguilera 2007) and will exacerbate transcriptional blocks imposed by positive supercoiling in the absence of Top1, Top2 and RNase H.

EM reveals polymerase pile-ups over the 5'-ETS and 5' region of 18S rDNA in the absence of Top1, RNase H1 and H201

To directly test the model that stable R-loops impose transcriptional blocks along the rDNA, we analyzed Pol I transcription by EM analysis of chromatin spreads. These were prepared from WT, P_{GAL} -*TOP1* (single mutant) and P_{GAL} -*TOP1 rnh1Δ rnh201Δ* (triple mutant) strains 6 hr after transfer to glucose medium at 30°C.

Inspection of Pol I distribution revealed the presence of “pile-ups”, which were defined as arrays of 5 or more polymerases with no visible intervening DNA (examples are bracketed in Fig. 6A). We attribute these to transcriptional pausing or stalling of the leading polymerase (situated

at the right-hand end of a bracket in Fig. 6A; see Fig. S6A for schematic), hindering the progression of subsequent polymerases. In WT cells, analysis of all visualized, active rDNA genes (data not shown) revealed pile-ups on 37% of genes (Number of genes analyzed = 105), showing that transient transcriptional pausing is surprisingly frequent. The fraction of genes showing pile-ups increased to 55% in the P_{GAL} - $TOP1$ single mutant (N = 180) and to 81% in the triple mutant (N = 209).

To determine whether polymerases were preferentially paused at particular sites, we divided the 35S gene into 20 equal segments and analyzed all genes that could be unambiguously traced from 5' to 3' ends. We mapped the position of the leading polymerase along a schematic 35S gene, in all pileups (≥ 5 polymerases; Fig. 6B) or in only longer pileups, which presumably reflect more persistent pauses (≥ 20 polymerases; Fig. S6B). Notably, the distribution of inferred pause sites along the rDNA was similar in all strains (Figs. 6B and S6B) indicating that pausing is a normal feature of Pol I transcription, which is exacerbated in the mutant strains. In WT, the major pause sites fell within the 18S rDNA, whereas lower levels of pausing were observed at sites in the 25S rDNA (Fig. 6B, blue). As Top1 was depleted pausing strongly increased along the 18S rDNA (Fig. 6B, red), and this was exacerbated when RNase H was also limiting (Fig. 6B, green). The increase in pausing was more prominent in the 5' region of the rDNA when both Top1 and RNase H were deficient, with stalled polymerases at the 5' region of 18S backed-up into the 5'-ETS. The proportion of 35S genes with pile-ups increased from WT to single to triple mutant strain (Fig. 6D). Both mutants showed similar numbers of polymerases per pile-up but this was greater than the WT (Fig. 6E).

Fig. 6B shows the locations of the leading polymerase in each pileup on active rDNA genes, but we also quantified the distribution of all polymerases (Fig. 6C). Pol I occupancy in the WT was predominant over the 5'-ETS and the 5' region of 18S (Fig. 6C, blue), consistent with Pol I ChIP data (compare blue graphs in Figs. 5A and 6C). In both mutants, Pol I occupancy increased from the promoter to $\sim +4000$ nt downstream (Fig. 6C red and green), with more polymerases across the 5'-ETS and 5' region of 18S in the triple mutant. The increase in pile-up frequency and Pol I occupancy (Figs. 6 B-C) together with the increased accumulation of RNA/DNA hybrids (Fig. 5B) across the 5'-ETS and 5' region of the 18S in the triple mutant suggested that stable R-loops exacerbate Pol I pausing in these regions. Persistent polymerase pile-ups are predicted to impose transcriptional blocks that would lead to reduced rRNA synthesis (Tous and Aguilera 2007; Klumpp and Hwa 2008), consistent with RNA analyses in the triple mutant (Fig. 4).

Gaps (DNA free of Pol I) were generally observed in front of pileups, but there was no clear correlation between the lengths of the pile-up and gap length (Fig. S7). This may simply reflect the stochastic nature of transcription initiation but might also indicate that paused polymerases impact on the elongation of neighboring polymerases. However, a complication is that the observed pileups presumably represent a mix of those in the process of formation, in which new polymerases are joining, and those in the process of resolution, in which previously stalled polymerases are moving away from the pause site.

In EM analyses the Pol I distribution observed in spreads of WT cells was in good agreement with the occupancy inferred from the ChIP data. The match was less close for P_{GAL} - $TOP1$ and P_{GAL} - $TOP1rh1\Delta rh201\Delta$ strains, but it should be noted that only polymerases on active genes are counted in EM analyses whereas ChIP efficiencies reflect the averaged distribution across all rDNA genes. Moreover, the efficiency of immunoprecipitation of crosslinked DNA fragments in ChIP analyses may not be fully proportional to the number of associated polymerases, since each fragment can be precipitated only once even if many polymerases are bound (for further discussion of this point see (Kim et al. 2009)).

R-loops associated with stalled polymerases were not visible in the chromatin spreads, suggesting that they may be limited in size by the subsequent polymerases. It is, however, unclear how R-loops would appear in chromatin spreads, or whether regions of rRNA genes harboring R-loops would be amenable to dispersal, since they may be subject to strong topological constraints.

We conclude that RNA Pol I frequently pauses or stalls during rDNA transcription even in wild-type strains, in particular over the 18S region. This could be caused by the accumulation of positive supercoils in front of the polymerase and/or R-loop formation in its wake. Pausing was greatly increased by loss of Top1 and further augmented when combined with reduced RNase H activity.

DISCUSSION

We report that pre-rRNA transcription is affected by the absence of Top1, particularly over the 5' region of 18S rDNA. Pre-rRNA fragments that accumulated in the absence of Top1 were consistent with cleavage of nascent transcripts. The truncated pre-rRNA fragments had predicted 5' ends at the transcription initiation site or at cotranscriptional cleavage site A₂ within ITS1 (Fig. 1A). The most abundant fragments extended from the initiation site into the 5' region of the 18S rRNA. Topoisomerase activity is essential for transcription by Pol I, since rRNA synthesis was abolished in *top2-ts top1Δ* mutants at 37°C (Brill et al. 1987; Schultz et al. 1992). We showed that in strains lacking both Top1 and Top2 transcription blockage predominantly occurs within the 18S 5' region (Figs. 3 and S4), again indicating the stringent requirement for topoisomerase activity in this region.

Negative torsion behind transcribing Pol I can lead to unpairing of the DNA helix followed by hybridization of the nascent pre-rRNA to the template strand, forming an R-loop (Drolet 2006; Aguilera and Gomez-Gonzalez 2008). R-loops are targets for RNase H, suggesting that this activity might generate pre-rRNA fragments observed in the absence of Top1 (see model Fig. 7). Consistent with this, decreased RNase H activity reduced pre-rRNA truncation in strains lacking Top1 (Fig. 4). rRNA synthesis was also reduced in these strains, supporting the conclusion from *in vitro* data (Tous and Aguilera, 2007) that stable R-loops block transcription elongation. Pre-rRNA fragment accumulation was not completely abolished in the absence of Top1 and RNase H1 and H201. This might reflect the residual RNase H activity in these strains (Arudchandran et al. 2000), intrinsic RNase H cleavage activity of A34/A49 heterodimer of RNA Pol I (Kuhn et al. 2007), endonuclease activity of the exosome subunit Rrp44 (Lebreton et al. 2008; Schaeffer et al. 2009; Schneider et al. 2009) or dissociation of the duplex by RNA-DNA helicases like Sen1 which plays a role in Pol I transcription termination (Kawauchi et al. 2008).

Truncated pre-rRNA fragments were stabilized in *top1Δ* strains defective in TRAMP (*trf4Δ*) or the exosome (*rrp6Δ*), indicating that these complexes degrade the 5' pre-rRNA fragments released by RNase H cleavage. The fate of the 3' fragments resulting from RNase H cleavage is unclear but rapid degradation by the nuclear 5' to 3' exonuclease Rat1 would be predicted. Rat1 functions in transcription termination at the 3' end of the rDNA (El Hage et al. 2008; Kawauchi et al. 2008) and might also play a role in the release of stalled polymerases associated with transcripts that are engaged in R-loops. Consistent with this model, Rat1 has been shown to function in termination of RNA Pol II molecules engaged in the production of uncapped mRNA (Jimeno-Gonzalez et al. 2010).

Strains carrying *rpa49Δ* and *rpa34Δ* are defective in Pol I elongation (Kuhn et al. 2007) and also accumulated pre-rRNA fragments that terminated in the 5' region of the 18S rDNA when combined with the exosome mutation *rrp6Δ* (data not shown), as previously seen in *rpa135(D784G) rrp6Δ* double mutants (Schneider et al., 2007). Thus, transcription through the 5' region of the 18S rDNA appears to pose a particular challenge to elongation-compromised Pol I. Moreover, pre-rRNA fragments with 3' ends that extended to the same region, were detected in TRAMP and exosome mutants with intact topoisomerase and RNA polymerase activity, indicating that some level of pre-rRNA truncation normally occurs here in wild-type strains.

In EM analyses, pile-ups of five or more polymerases were seen on 37% of active WT rDNA transcription units, principally over the 18S rDNA. We interpret these as resulting from the collision of multiple transcribing polymerases with a single stalled or paused Pol I. In strains lacking Top1 the proportion of rDNA units with stalled Pol I was increased to 53%, and this rose to 84% in strains lacking both Top1 and RNase H. Notably, the distribution of the leading stalled polymerase was not clearly altered in the different strains, suggesting that the loss of these activities exacerbates an underlying pause that is present in the wild-type. In the absence of Top1 both the frequency of pile-ups and the numbers of contiguous polymerases increased, presumably reflecting increased duration of stalling of the leading polymerase. In strains lacking both Top1 and RNase H activity, pile-up frequency further increased. The presence of persistent R-loops might slow down local rotation of the rDNA reducing the speed of elongation of Pol I in the same pile-up, which would increase the residency times of pile-ups and impede their resolution (see model Fig. 7). The density of R-loops was dramatically increased in strains lacking both Top1 and RNase H activity, particularly over the promoter and 5'-ETS region (Fig.5). This may reflect both the increased time available for R-loop formation, due to the stalled polymerases, and R-loop stabilization due to reduced RNase H activity.

The similarities in the distribution of stalled Pol I, R-loops and pre-rRNA cleavage sites suggest that underlying features of transcription in the 5' region of the 18S rDNA are distinct from other segments of the 6.7Kb pre-rRNA transcript. This region lies ~1Kb, or around 100 turns of the rDNA, from the start of transcription, and it is feasible that, simply due to physical features of transcription, Top1 activity first becomes crucial for Pol I transcription over this region. However, the existence of a check-point for ribosome assembly, which would slow Pol I elongation until the pre-rRNA is folded and/or bound by r-proteins and pre-40S assembly factors, was previously suggested (Moss et al. 2007; Schneider et al. 2007). In yeast, the U3 snoRNA binds to the 5'-ETS and to the extreme 5' end of the 18S rRNA sequence, where it may play a major role in the mechanism or timing of formation of the central pseudoknot in 18S rRNA

(reviewed in (Henras et al. 2008)). It could be envisaged that binding and/or release of U3 and other early-acting ribosome synthesis factors is synchronized with the transcription elongation rate to promote productive pre-rRNA folding and reduce the tendency of exposed, unfolded RNA sequences to generate R-loops. Such surveillance of pre-ribosome assembly might preferentially occur at a location where Pol I is slowed by physical processes.

In the absence of Top1, levels of Pol II ncRNA transcripts derived from the rDNA intergenic spacer regions (IGS) and rDNA recombination are both increased relative to WT strains (Bryk et al. 1997; Houseley et al. 2007). We speculate that under-wound DNA in the IGS regions disrupts transcriptional silencing and forms R-loops with ncRNAs, which might be poorly packaged. This leaves the complementary strand single-stranded and prone to cleavage and recombination (Aguilera and Gomez-Gonzalez 2008). In strains lacking Top1 and RNase H, RNA-DNA hybrids accumulated over IGS1 and IGS2 and ncRNA levels were increased relative to *top1* Δ single mutants, suggesting that RNase H-mediated cleavage is a major pathway of ncRNA degradation in the *top1* Δ strains.

In yeast, cleavage of the nascent transcripts generated by RNA Pol II is essential to avoid transcriptional road-blocks and for cell viability (Sigurdsson et al. 2010). Similarly, cleavage of the pre-rRNA in *top1* Δ and Pol I elongation mutants might be essential to avoid transcriptional blocks, in particular over the 5' region of 18S. Persistent accumulation of Pol I pile-ups along the rDNA was also predicted to reduce rRNA transcription in modeling data from Bacteria (Klumpp and Hwa 2008). R-loop formation also occurs in topoisomerase I mutants in *E.coli* and leads to growth defects, impaired transcription elongation on the rDNA and extensive RNA degradation by RNase H (Hraiky et al. 2000; Drolet 2006; Baaklini et al. 2008). This supports the conclusion (Li and Manley 2006) that the deleterious effects that R-loops can have on transcription have been conserved over a long evolutionary distance.

Materials and Methods

Strains, plasmids and growth conditions

All mutants and tagged yeast strains were constructed using strain BY4741 (derived from S288C). Strains and plasmids used in this study are listed in Table S1 available with this article online. Regulated P_{GAL} expression and deletions were constructed by one-step PCR using template plasmids pFA6a-kanMX6-PGAL1-3HA and pFA6a-kanMX6/NatMX6/HphMX6, respectively. Growth and handling of *S.cerevisiae* were by standard techniques. Cells were grown in YPD medium at 18°C, 25°C or 30°C. For RNA and ChIP analyses, strains where *TOP1* or *TOP2* were placed under P_{GAL1} promoter were grown at 30°C to $OD_{600} \sim 0.3-0.4$ in complete synthetic medium containing 2% galactose and 2% sucrose then transferred to the same pre-warmed medium containing 2% glucose. For EM analysis WT, P_{GAL} -*TOP1* and P_{GAL} -*TOP1 rnh1Δ rnh201Δ* strains were grown at 30°C in YP-Gal then shifted to YPD for 6 hr.

RNA Analyses

RNA extraction, Northern hybridization and quantifications were as described (El Hage et al. 2008) and Supp. Methods. PolyA RNA extraction was as described (Dez et al. 2006) and Supp. Methods. Primers for RNA analysis are listed in Table S2.

Chromatin immunoprecipitation (ChIP)

ChIP experiments were performed essentially as described (El Hage et al. 2008) and Supp. Methods. RNA-DNA hybrids were detected using Ab S9.6 kindly provided by Dr. S. Leppla, or purified by Eurogentec from supernatants of mouse hybridoma cell line purchased from ATCC. Pol I subunit Rpa190 was detected with Rabbit polyclonal antibody (Kind gift from David Schneider). Pol I subunit Rpa34-13MYC was detected using Mouse monoclonal antibody c-Myc 9E11 (Santa Cruz). Primers used for Q-PCRs are listed in Table S3.

For detection of both RNA-DNA hybrids and Rpa190 in Fig.5, sonicated DNA from the same strain was split in 3 equal parts that served for no-antibody control, S9.6 and anti-Rpa190. Values for ChIPs were determined using the formula $\Delta Ct = 2^{-(Ct IP - Ct Background)}$. “Ct IP” is the cycle number for immunoprecipitate and “Ct Background” is the cycle number for control without antibody. To normalize Pol I ChIP values for Figs. 5A and D, each set of Rpa190- ΔCt values were normalized to 25S (=average of ΔCt values of primers **j** and **k**) in the same dataset. The means of 3-5 independent experiments (replicates) were calculated with standard error. This shows the relative distribution of Pol I along the length of the rDNA in each strain. However, because the values are internally normalized, differences in overall Pol I ChIP signals between

different strains will be lost. To assess this, we divided the average of the Rpa190- Δ Ct values from each mutant to the average of the Rpa190- Δ Ct values from the WT. The normalized ChIP values obtained for each dataset for the mutants were then multiplied by this correction factor.

A different correction was applied in Figs. 5B and E to account for differences in ChIP efficiencies and Pol I loading. The Δ Ct values for RNA/DNA hybrids were each normalized to the average of Rpa190- Δ Cts within the same strain and replicate. The means of 3-5 independent experiments were calculated with standard error

Electron Microscopy

Miller chromatin spreads and EM analyses were performed as described (Osheim et al. 2009) and Supp. Methods.

ACKNOWLEDGEMENTS

We thank Steven Lepla, David Schneider, Andrés Aguilera and Brian Luke for providing reagents. We thank Jean Beggs, Steve Innocente, Laura Milligan and Olivier Cordin for fruitful discussions, Lea Harrington and Laura Guardano for helping with the production of S9.6 antibodies, and Alexandra Moreira and Steve West for critical reading of the manuscript. This work was supported by the Wellcome Trust and by US Public Health Service grant GM-63952 to ALB.

REFERENCES

- Aguilera, A. and Gomez-Gonzalez, B. 2008. Genome instability: a mechanistic view of its causes and consequences. *Nat Rev Genet* **9**(3): 204-217.
- Arudchandran, A., Cerritelli, S., Narimatsu, S., Itaya, M., Shin, D.Y., Shimada, Y., and Crouch, R.J. 2000. The absence of ribonuclease H1 or H2 alters the sensitivity of *Saccharomyces cerevisiae* to hydroxyurea, caffeine and ethyl methanesulphonate: implications for roles of RNases H in DNA replication and repair. *Genes Cells* **5**(10): 789-802.
- Baaklini, I., Usongo, V., Nolent, F., Sanscartier, P., Hraiky, C., Drlica, K., and Drolet, M. 2008. Hypernegative supercoiling inhibits growth by causing RNA degradation. *J Bacteriol* **190**(22): 7346-7356.
- Beckouet, F., Labarre-Mariotte, S., Albert, B., Imazawa, Y., Werner, M., Gadai, O., Nogi, Y., and Thuriaux, P. 2008. Two RNA polymerase I subunits control the binding and release of Rrn3 during transcription. *Mol Cell Biol* **28**(5): 1596-1605.
- Boguslawski, S.J., Smith, D.E., Michalak, M.A., Mickelson, K.E., Yehle, C.O., Patterson, W.L., and Carrico, R.J. 1986. Characterization of monoclonal antibody to DNA.RNA and its application to immunodetection of hybrids. *J Immunol Methods* **89**(1): 123-130.

- Brill, S.J., DiNardo, S., Voelkel-Meiman, K., and Sternglanz, R. 1987. Need for DNA topoisomerase activity as a swivel for DNA replication for transcription of ribosomal RNA. *Nature* **326**(6111): 414-416.
- Bryk, M., Banerjee, M., Murphy, M., Knudsen, K.E., Garfinkel, D.J., and Curcio, M.J. 1997. Transcriptional silencing of Ty1 elements in the RDN1 locus of yeast. *Genes Dev* **11**(2): 255-269.
- Cook, P.R. 1999. The organization of replication and transcription. *Science* **284**(5421): 1790-1795.
- Dez, C., Houseley, J., and Tollervey, D. 2006. Surveillance of nuclear-restricted pre-ribosomes within a subnucleolar region of *Saccharomyces cerevisiae*. *Embo J* **25**(7): 1534-1546.
- Drolet, M. 2006. Growth inhibition mediated by excess negative supercoiling: the interplay between transcription elongation, R-loop formation and DNA topology. *Mol Microbiol* **59**(3): 723-730.
- El Hage, A., Koper, M., Kufel, J., and Tollervey, D. 2008. Efficient termination of transcription by RNA polymerase I requires the 5' exonuclease Rat1 in yeast. *Genes Dev* **22**(8): 1069-1081.
- French, S.L., Osheim, Y.N., Cioci, F., Nomura, M., and Beyer, A.L. 2003. In exponentially growing *Saccharomyces cerevisiae* cells, rRNA synthesis is determined by the summed RNA polymerase I loading rate rather than by the number of active genes. *Mol Cell Biol* **23**(5): 1558-1568.
- French, S.L., Sikes, M.L., Hontz, R.D., Osheim, Y.N., Lambert, T.E., Hage, A.E., Smith, M.M., Tollervey, D., Smith, J.S., and Beyer, A.L. submitted. Distinguishing the roles of Topoisomerase I and II in relief of transcription-induced torsional stress in yeast rDNA genes.
- Henras, A.K., Soudet, J., Gerus, M., Lebaron, S., Caizergues-Ferrer, M., Mougin, A., and Henry, Y. 2008. The post-transcriptional steps of eukaryotic ribosome biogenesis. *Cell Mol Life Sci* **65**(15): 2334-2359.
- Houseley, J., Kotovic, K., El Hage, A., and Tollervey, D. 2007. Trf4 targets ncRNAs from telomeric and rDNA spacer regions and functions in rDNA copy number control. *Embo J* **26**(24): 4996-5006.
- Hraiky, C., Raymond, M.A., and Drolet, M. 2000. RNase H overproduction corrects a defect at the level of transcription elongation during rRNA synthesis in the absence of DNA topoisomerase I in *Escherichia coli*. *J Biol Chem* **275**(15): 11257-11263.
- Hu, Z., Zhang, A., Storz, G., Gottesman, S., and Leppla, S.H. 2006. An antibody-based microarray assay for small RNA detection. *Nucleic Acids Res* **34**(7): e52.
- Huertas, P. and Aguilera, A. 2003. Cotranscriptionally formed DNA:RNA hybrids mediate transcription elongation impairment and transcription-associated recombination. *Mol Cell* **12**(3): 711-721.
- Jeong, H.S., Backlund, P.S., Chen, H.C., Karavanov, A.A., and Crouch, R.J. 2004. RNase H2 of *Saccharomyces cerevisiae* is a complex of three proteins. *Nucleic Acids Res* **32**(2): 407-414.
- Jimeno-Gonzalez, S., Haaning, L.L., Malagon, F., and Jensen, T.H. 2010. The yeast 5'-3' exonuclease Rat1p functions during transcription elongation by RNA polymerase II. *Mol Cell* **37**(4): 580-587.
- Kawauchi, J., Mischo, H., Braglia, P., Rondon, A., and Proudfoot, N.J. 2008. Budding yeast RNA polymerases I and II employ parallel mechanisms of transcriptional termination. *Genes Dev* **22**(8): 1082-1092.
- Kim, M., Suh, H., Cho, E.J., and Buratowski, S. 2009. Phosphorylation of the yeast Rpb1 C-terminal domain at serines 2, 5, and 7. *J Biol Chem* **284**(39): 26421-26426.

- Klumpp, S. and Hwa, T. 2008. Stochasticity and traffic jams in the transcription of ribosomal RNA: Intriguing role of termination and antitermination. *Proc Natl Acad Sci U S A* **105**(47): 18159-18164.
- Kos, M. and Tollervey, D. 2010. Yeast Pre-rRNA Processing and Modification Occur Cotranscriptionally. *Mol Cell* **37**(6): 809-820.
- Koster, D.A., Palle, K., Bot, E.S., Bjornsti, M.A., and Dekker, N.H. 2007. Antitumour drugs impede DNA uncoiling by topoisomerase I. *Nature* **448**(7150): 213-217.
- Kuhn, C.D., Geiger, S.R., Baumli, S., Gartmann, M., Gerber, J., Jennebach, S., Mielke, T., Tschochner, H., Beckmann, R., and Cramer, P. 2007. Functional architecture of RNA polymerase I. *Cell* **131**(7): 1260-1272.
- Lavelle, C. 2008. DNA torsional stress propagates through chromatin fiber and participates in transcriptional regulation. *Nat Struct Mol Biol* **15**(2): 123-125.
- Lebreton, A., Tomecki, R., Dziembowski, A., and Seraphin, B. 2008. Endonucleolytic RNA cleavage by a eukaryotic exosome. *Nature* **456**(7224): 993-996.
- Li, C., Mueller, J.E., and Bryk, M. 2006. Sir2 represses endogenous polymerase II transcription units in the ribosomal DNA nontranscribed spacer. *Mol Biol Cell* **17**(9): 3848-3859.
- Li, X. and Manley, J.L. 2005. Inactivation of the SR protein splicing factor ASF/SF2 results in genomic instability. *Cell* **122**(3): 365-378.
- . 2006. Cotranscriptional processes and their influence on genome stability. *Genes Dev* **20**(14): 1838-1847.
- Luke, B., Panza, A., Redon, S., Iglesias, N., Li, Z., and Lingner, J. 2008. The Rat1p 5' to 3' Exonuclease Degrades Telomeric Repeat-Containing RNA and Promotes Telomere Elongation in *Saccharomyces cerevisiae*. *Mol Cell* **32**(4): 465-477.
- Moss, T., Langlois, F., Gagnon-Kugler, T., and Stefanovsky, V. 2007. A housekeeper with power of attorney: the rRNA genes in ribosome biogenesis. *Cell Mol Life Sci* **64**(1): 29-49.
- Osheim, Y.N., French, S.L., Keck, K.M., Champion, E.A., Spasov, K., Dragon, F., Baserga, S.J., and Beyer, A.L. 2004. Pre-18S ribosomal RNA is structurally compacted into the SSU processome prior to being cleaved from nascent transcripts in *Saccharomyces cerevisiae*. *Mol Cell* **16**(6): 943-954.
- Osheim, Y.N., French, S.L., Sikes, M.L., and Beyer, A.L. 2009. Electron Microscope Visualization of RNA Transcription and Processing in *Saccharomyces cerevisiae* by Miller Chromatin Spreading. *Methods Mol Biol* **464**: 55-69.
- Roy, D., Zhang, Z., Lu, Z., Hsieh, C.L., and Lieber, M.R. 2009. Competition between the RNA transcript and the nontemplate DNA strand during R-loop formation in vitro: a nick can serve as a strong R-loop initiation site. *Mol Cell Biol* **30**(1): 146-159.
- Schaeffer, D., Tsanova, B., Barbas, A., Reis, F.P., Dastidar, E.G., Sanchez-Rotunno, M., Arraiano, C.M., and van Hoof, A. 2009. The exosome contains domains with specific endoribonuclease, exoribonuclease and cytoplasmic mRNA decay activities. *Nat Struct Mol Biol* **16**(1): 56-62.
- Schneider, C., Leung, E., Brown, J., and Tollervey, D. 2009. The N-terminal PIN domain of the exosome subunit Rrp44 harbors endonuclease activity and tethers Rrp44 to the yeast core exosome. *Nucleic Acids Res* **37**(4): 1127-1140.
- Schneider, D.A., Michel, A., Sikes, M.L., Vu, L., Dodd, J.A., Salgia, S., Osheim, Y.N., Beyer, A.L., and Nomura, M. 2007. Transcription elongation by RNA polymerase I is linked to efficient rRNA processing and ribosome assembly. *Mol Cell* **26**(2): 217-229.
- Schultz, M.C., Brill, S.J., Ju, Q., Sternglanz, R., and Reeder, R.H. 1992. Topoisomerases and yeast rRNA transcription: negative supercoiling stimulates initiation and topoisomerase activity is required for elongation. *Genes Dev* **6**(7): 1332-1341.
- Sigurdsson, S., Dirac-svejstrup, A.B., and Svejstrup, J.Q. 2010. Evidence that Transcript Cleavage is Essential for RNA Polymerase II Transcription and Cell Viability. *Molecular Cell* **38**: 202-210.

- Sutherland, H. and Bickmore, W.A. 2009. Transcription factories: gene expression in unions? *Nat Rev Genet* **10**(7): 457-466.
- Tous, C. and Aguilera, A. 2007. Impairment of transcription elongation by R-loops in vitro. *Biochem Biophys Res Commun* **360**(2): 428-432.
- Trigueros, S. and Roca, J. 2002. Failure to relax negative supercoiling of DNA is a primary cause of mitotic hyper-recombination in topoisomerase-deficient yeast cells. *J Biol Chem* **277**(40): 37207-37211.
- Tuduri, S., Crabbe, L., Conti, C., Tourriere, H., Holtgreve-Grez, H., Jauch, A., Pantesco, V., De Vos, J., Thomas, A., Theillet, C., Pommier, Y., Tazi, J., Coquelle, A., and Pasero, P. 2009. Topoisomerase I suppresses genomic instability by preventing interference between replication and transcription. *Nat Cell Biol*.
- Wang, J.C. 2002. Cellular roles of DNA topoisomerases: a molecular perspective. *Nat Rev Mol Cell Biol* **3**(6): 430-440.
- Wang, J.C. and Lynch, A.S. 1993. Transcription and DNA supercoiling. *Curr Opin Genet Dev* **3**(5): 764-768.
- Wery, M., Ruidant, S., Schillewaert, S., Lepore, N., and Lafontaine, D.L. 2009. The nuclear poly(A) polymerase and Exosome cofactor Trf5 is recruited cotranscriptionally to nucleolar surveillance. *RNA* **15**(3): 406-419.
- Zhang, H., Wang, J.C., and Liu, L.F. 1988. Involvement of DNA topoisomerase I in transcription of human ribosomal RNA genes. *Proc Natl Acad Sci U S A* **85**(4): 1060-1064.
- Zhang, Y., Sikes, M.L., Beyer, A.L., and Schneider, D.A. 2009. The Paf1 complex is required for efficient transcription elongation by RNA polymerase I. *Proc Natl Acad Sci U S A* **106**(7): 2153-2158.

FIGURE LEGENDS

Figure 1. Aberrant pre-rRNAs generated in the absence of Top1 are targeted for degradation by TRAMP and exosome complexes

(A) Schematic representation of a 35S rRNA gene in *S.cerevisiae*. Pre-rRNA processing sites A0, A1, D, A2, A3, B1, C2, C1, B2 and B0 are labeled. Probes used in northern analyses are indicated by bars. The 35S, 20S, 27SA and 27SB pre-rRNAs are depicted by solid arrows. Truncated pre-rRNA fragments generated in the absence of Top1 are depicted by dotted arrows and labeled 1-9. Numbers of nucleotides along the rDNA unit relative to the start of transcription (0) are indicated. The pre-rRNA processing pathway is depicted in Fig. S1.

(B-E) Polyadenylated pre-rRNA fragments accumulate in double *top1Δ rrp6Δ* mutants. Total RNA was extracted from WT, *rrp6Δ*, *top1Δ* and *top1Δ rrp6Δ* strains grown at 25°C. Polyadenylated RNAs were purified and resolved alongside total RNAs on a 1.2% glyoxal-agarose gel. Pre-rRNA fragments were detected by northern analysis: (B) probe 033 hybridizing at +278 in 5'-ETS, (C) probe 004, hybridizing upstream of site A2 and (D) probe 003 hybridizing between A2 and A3. (E) As controls for poly(A)⁺ RNA specificity, 25S and 18S rRNA and PGK1 mRNA were analyzed. (F-G) TRAMP participates in pre-rRNA surveillance in *top1Δ* mutants. Total RNA was extracted from WT, single and double *top1Δ*, *trf4Δ* and *rrp6Δ* strains grown at 25°C and analyzed using probe 130 (hybridizes in the 5'-ETS upstream of probe 033) and 003. F and G are from two independent experiments. SCR1 was used as a loading control (bottom panels). Intact pre-rRNAs and truncated pre-rRNA fragments are labeled. (18S) and (25S) indicate the positions of migration of 18S and 25S rRNAs. Probe names are bracketed. The 23S RNA is an aberrant pre-rRNA processing intermediate extending from +1 to site A3, previously shown to be polyadenylated and targeted for degradation by TRAMP and Rrp6 (Dez et al., 2006).

Figure 2. Pre-rRNA synthesis defects increase in *top1Δ* mutant at low growth temperatures

Total RNA from WT and single *top1Δ* strain grown at 18°C, 25°C or 30°C was resolved on an agarose gel and analyzed by northern hybridization, using probes 130 (A), 003 (B, C and E) and 004 (D). (F) Cytoplasmic SCR1 RNA was used as a loading control. C shows a stronger exposure of the lower region (below 18S) of B. Intact pre-rRNAs and truncated pre-rRNA fragments are labeled. (18S) and (25S) indicate the position of migration of 18S and 25S rRNAs. Probe names are bracketed (see Fig. 1A for location of probes).

Figure 3. Pre-rRNAs are predominately truncated within the 5' region of 18S rRNA when both Top1 and Top2 are absent

(A) Diagram representing the 5'-ETS and 18S rDNA sequences. Heterogeneous, truncated pre-rRNA fragments that accumulate in the absence of both Top1 and Top2 are depicted by dotted arrows followed by a star.

(B-H) Strains $P_{GAL-TOP2}$ and $P_{GAL-TOP2} top1\Delta$ were shifted from galactose (0 hr) to glucose containing medium at 30°C (2-10 hr). Total RNA was analyzed by northern hybridization. The membrane was hybridized successively with probes 130 (B), 004 (C), 003 (D), 008 (F) and 007 (G). Random primed probe IGS2 (E) was used to detect ncRNAs transcribed by RNA Pol II from the intergenic rDNA spacers IGS1 and IGS2, located between the 35S rDNA units. Cytoplasmic SCR1 RNA (H) was used as a loading control. Intact pre-rRNAs and truncated pre-rRNA fragments are labeled. Heterogeneous truncated pre-rRNA fragments are labeled by stars. (18S) and (25S) indicate the position of migration of 18S and 25S rRNAs. Probe names are bracketed (see Fig. 1A for location of probes).

Figure 4. RNase H facilitates pre-rRNA transcription in the absence of Top1

(A) Schematic showing the locations of pre-rRNAs (solid arrows), truncated pre-rRNA fragments (dashed arrows, left), and RNA Pol II transcribed ncRNAs synthesized from the intergenic spacer regions (dashed arrows, right).

(B-J) Strains $P_{GAL-TOP1}$ and $P_{GAL-TOP1} rnh1\Delta rnh201\Delta$ were shifted from galactose (0 hr) to glucose containing medium at 30°C (2-14 hr). Total RNA was analyzed by northern hybridization. The membrane was hybridized successively with probes 130 (B), 003 (C and E) and 004 (D). SCR1 (F) was used as a loading control. Random primed probe IGS2 (G) was used to detect ncRNAs transcribed from the intergenic rDNA spacers IGS1 and IGS2. (H) Ethidium staining of 25S and 18S rRNAs. Intact pre-rRNAs and truncated pre-rRNA fragments are labeled. (18S) and (25S) indicate the position of migration of 18S and 25S rRNAs. Probe names are bracketed (see Fig. 1A for locations of probes). (I and J) Quantification of 20S and 27S pre-rRNAs detected by probes 004 (D) and 003 (E). Signals were normalized to the loading control SCR1 (F) and expressed relative to 0 hr samples, which were set to 1.

Figure 5. ChIP analyses of Pol I and RNA/DNA hybrids over the rDNA unit

ChIP analyses of the occupancy of Pol I (A and D) and RNA/DNA hybrids (B and E) over the rDNA were performed at 6 hr after shift from galactose to glucose containing media at 30°C, using a combination of either WT, $P_{GAL-TOP1}$ and $P_{GAL-TOP1} rnh1\Delta rnh201\Delta$ strains (A-B) or

WT, $P_{GAL}\text{-TOP1 } P_{GAL}\text{-TOP2}$ and $P_{GAL}\text{-TOP1 } P_{GAL}\text{-TOP2 } rnh1\Delta rnh201\Delta$ strains (**D-E**). Sonicated-crosslinked-chromatin from each strain served for the immunoprecipitation of Pol I (Rpa190) and RNA/DNA hybrids (**A,D** and **B,E**). Numbers of base pairs along the rDNA unit relative to the start of 35S rRNA transcription (0) are plotted on the X axis. The middle position of each PCR fragment quantified is plotted below the X axis and indicated by a letter (**a** to **p**; for coordinates of QPCR primers Table S3). An rDNA cartoon is shown below each graph, with the promoter and terminator depicted by an arrow and a lollipop, respectively. The means of 3-5 independent experiments are shown with standard error. Relative ChIP signals are plotted on the Y axis (for normalizations see Materials and Methods). (**C**) Schematic representation of the ribosome assembly pathway as visualized by EM Miller spreads of active rDNA genes adapted from Fig. 8 in (Wery et al. 2008); see also (Osheim et al. 2004). Filled and empty triangles represent pre-ribosomal proteins and synthesis factors assembling cotranscriptionally into nascent pre-ribosomes. Cleavage at site A2 is indicated above the 25S gene. The EM image shows an rRNA gene from a *top1* Δ strain.

Figure 6. Polymerase pile-ups over the 5'-ETS and 18S increase when Top1, RNase H1 and H201 are absent

(**A**) Representative rRNA genes from Miller spreads of WT, $P_{GAL}\text{-TOP1}$ and $P_{GAL}\text{-TOP1 } rnh1\Delta rnh201\Delta$ strains after 6 hr of Top1 depletion in glucose at 30°C. Brackets indicate sites of polymerase pile-ups. These were defined as at least 5 tightly packed polymerases. The leading polymerase corresponds to the polymerase situated at the right-hand end of a bracket (Fig. S6A).

(**B**) Sites of Pol I pausing across the 35S rDNA gene. The gene was divided into 20 equal segments (~337 bp each) and the position of the leading polymerase in each pile-up was plotted onto the segment in which it occurred. The Y axis shows the percentage of all rDNA genes for each strain with a pile-up starting at the indicated position along the gene (X axis). All rDNA genes that could be visualized from the 5' to 3' end were included in the analysis and their lengths were normalized.

(**C**) EM analysis of Pol I occupancy over the rDNA unit. For each of the 3 strains, polymerase positions were measured along 77 rDNA genes, yielding the position of 15,115 polymerases. Each gene was divided into 20 equal segments, and the number of polymerases in each segment was determined. Data were plotted using the midpoints of the 20 gene segments for positioning on the X-axis using smoothed lines.

(**D**) Total frequencies of pileup occurrence for WT and mutant strains. N = number of rDNA

genes analyzed. The same sample of genes was used in **B**.

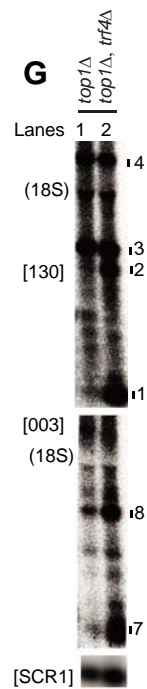
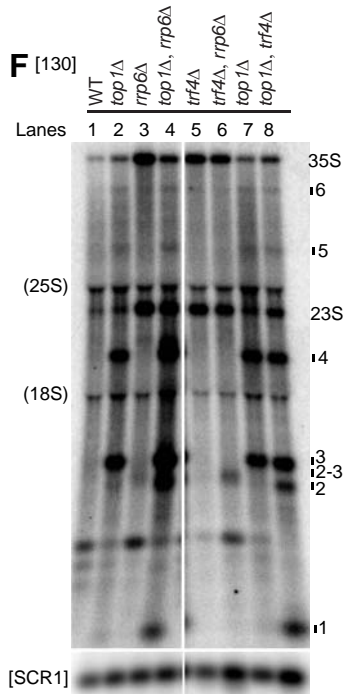
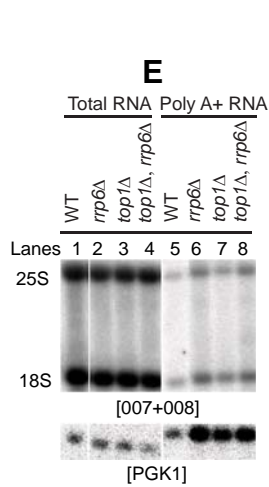
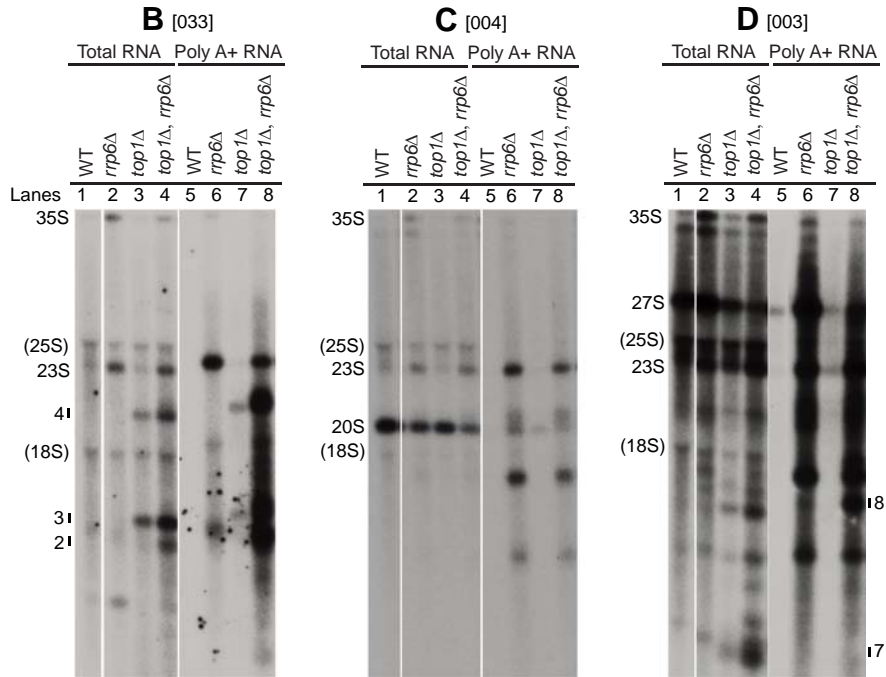
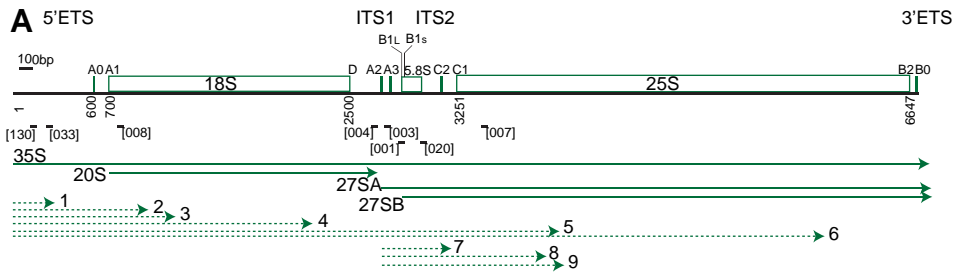
(**E**) Plot of pile-up lengths (number of polymerases per pileup) for WT and mutant strains. The same sample of genes was used in **B**.

Figure 7. Model for the role of R-loops in blocking pre-rRNA transcription

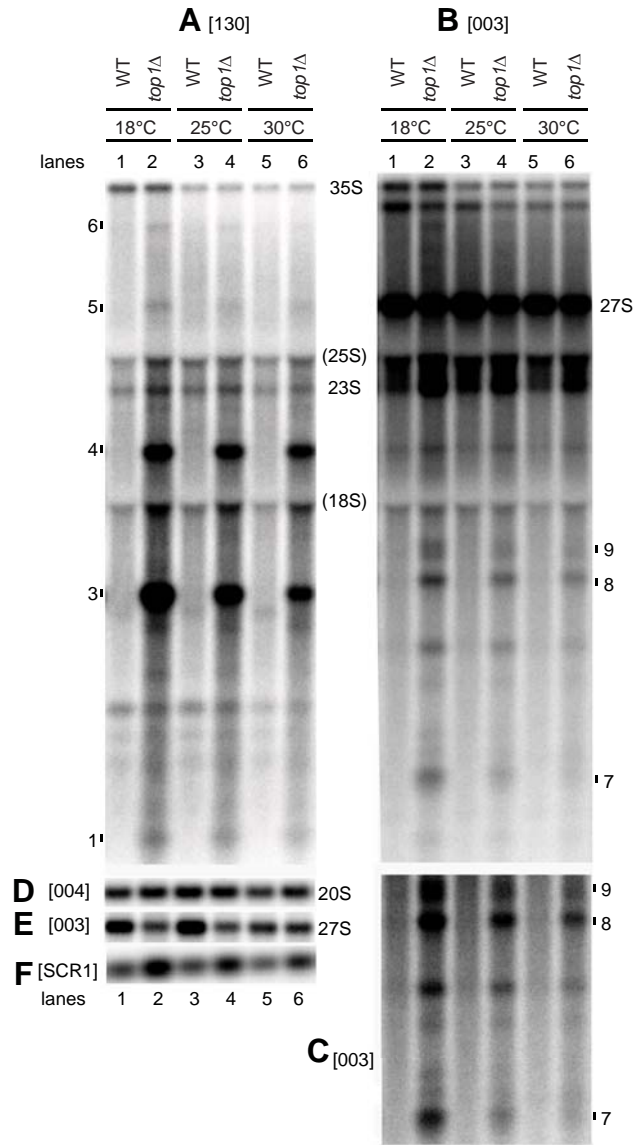
(**A**) Polymerase movement during transcription forces the rDNA to rotate building-up positive torsion (+) in front and negative torsion (-) in its rear (Cook 1999). Torsion ahead of Pol I causes positive supercoiling, which resist strand opening. This slows or pauses transcription elongation generating polymerase pileups, in particular over the 5' region of the 18S rDNA. Torsion behind the polymerase leads to negative supercoiling, which facilitates DNA strand opening and stimulates formation of R-loops with the nascent pre-rRNA (Roy et al. 2009). These structures also slow transcription elongation (Tous and Aguilera 2007) and trigger pile-up formation. In WT strains, pileups are normally transient, with Top1 resolving both negative and positive supercoiling and facilitating transcription. rDNA rotation and direction of transcription are depicted by a bent and a straight arrow, respectively.

(**B**) In strains lacking Top1, which provides the major topoisomerase activity during rDNA transcription, more torsion is accumulated (-- and ++) and R-loops occur more frequently, leading to an increase in pile-up formation. RNase H1 and H2 cleave the RNA-DNA hybrids, releasing truncated pre-rRNA fragments that are targeted and degraded by the TRAMP and exosome complexes. Top2 resolves positive and negative supercoiling. Both activities should lead to the release of transcriptional blocks but Top2 is not predicted to resolve strand separation induced by negative torsion (Lavelle 2008; French et al. submitted).

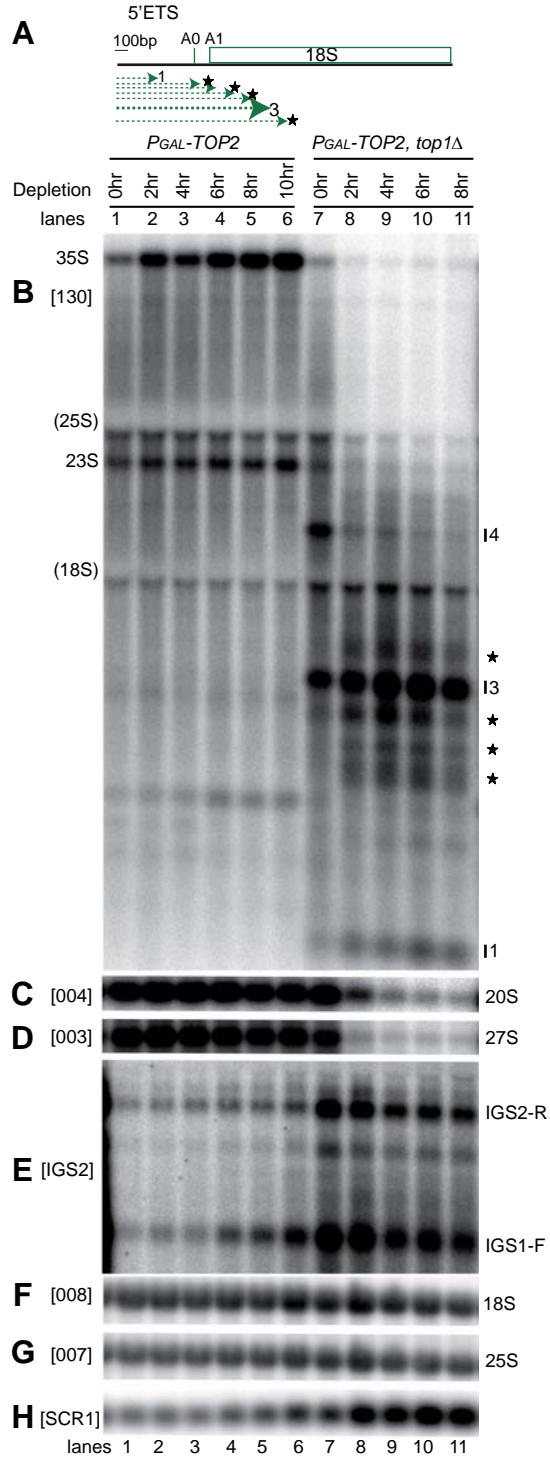
(**C**) In the absence of both Top1 and RNase H1 and H201, persistent R-loops block rotation of the rDNA and cause severe polymerase arrests and pile-ups.

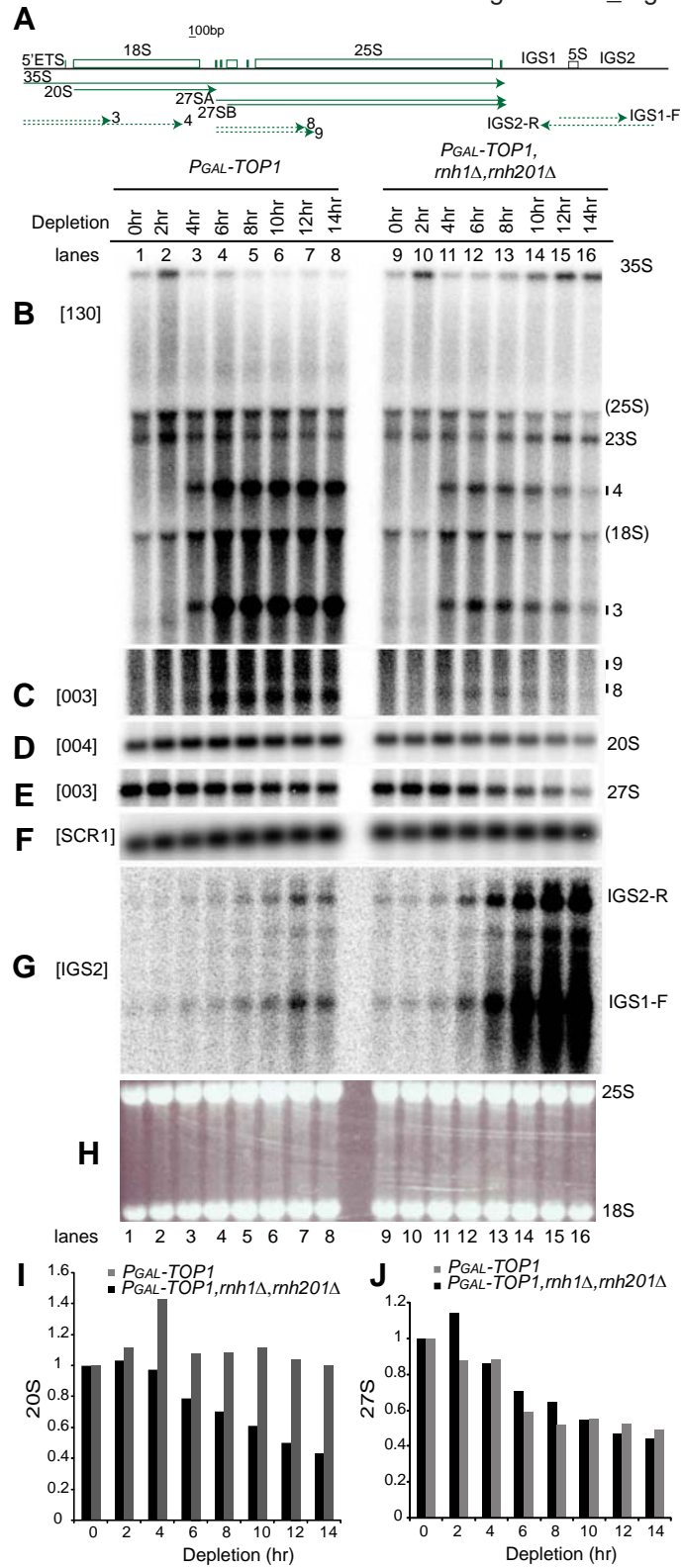


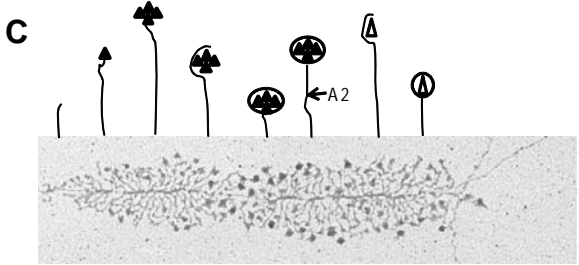
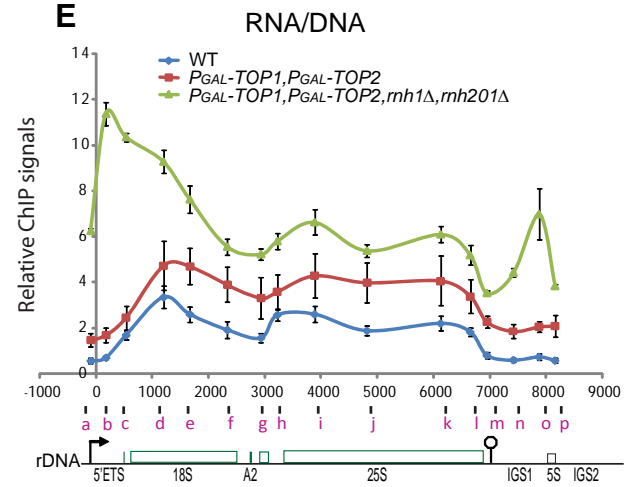
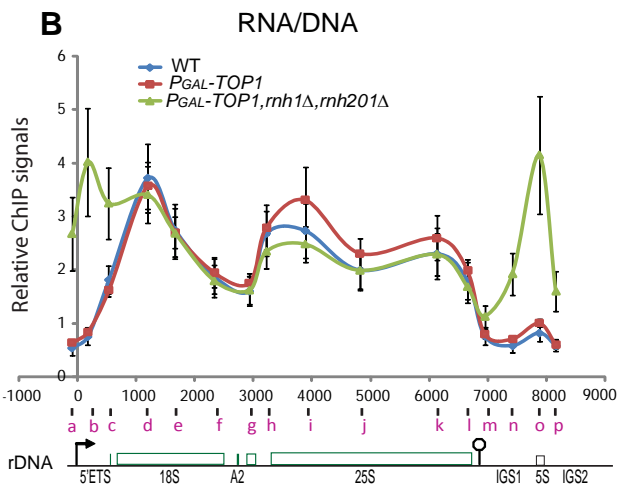
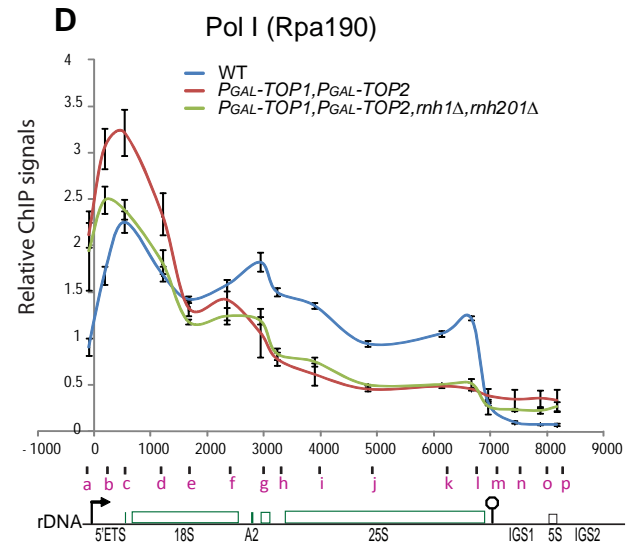
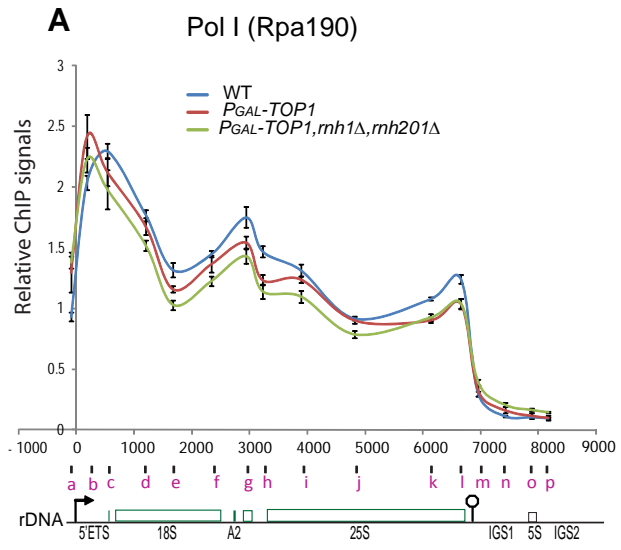
El Hage138248_Fig2

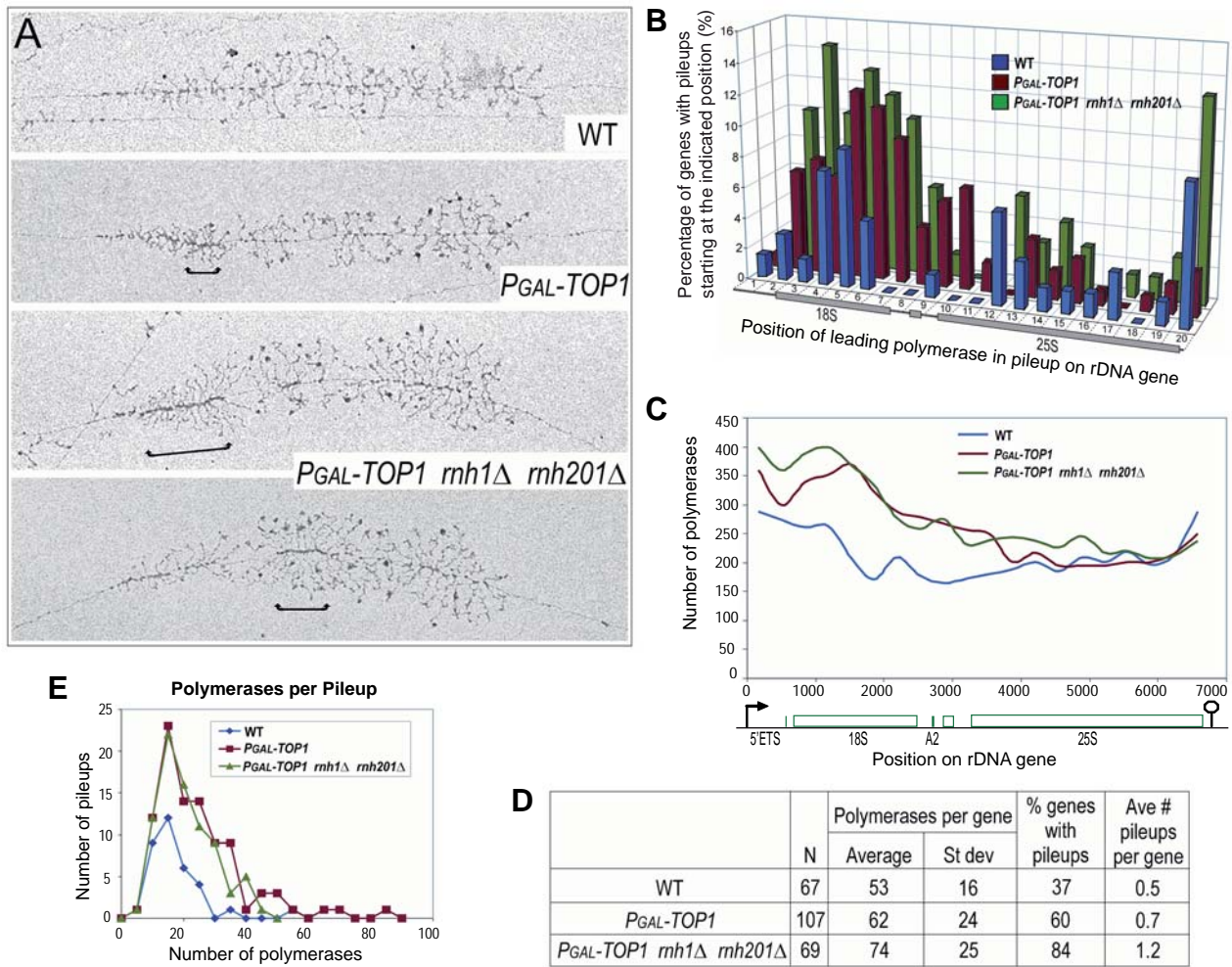


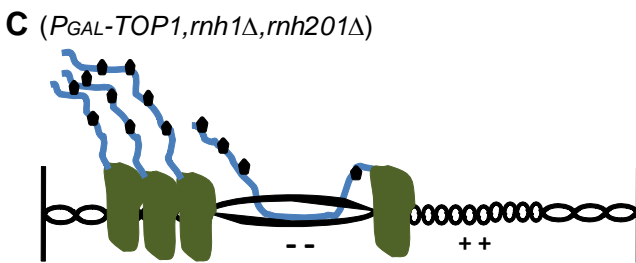
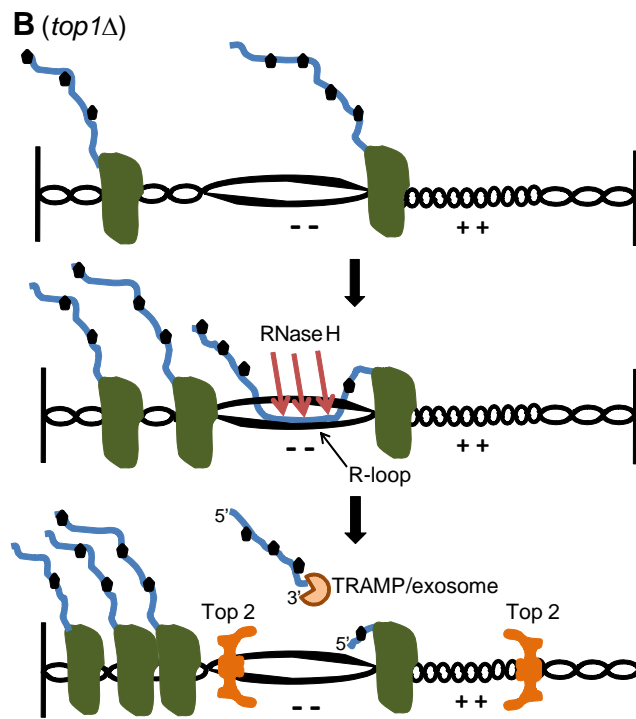
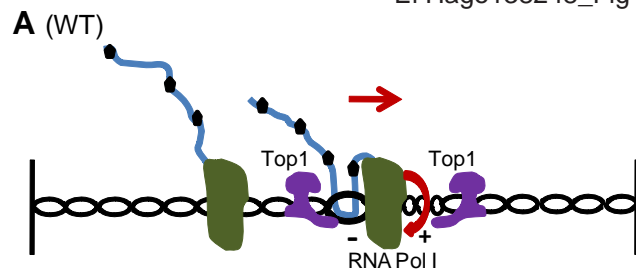
El Hage138248_Fig3











Supplementary Material

Figure S1. Major rRNA maturation pathway in *S.cerevisiae*.

The 35S pre-rRNA is cleaved at processing sites A0, A1 and A2 either co-transcriptionally on the nascent transcript, or post-transcriptionally; see (Osheim et al. 2004; Kos and Tollervey 2010; Warner and Kim 2010). The 5' cleavage product is 20S pre-rRNA, which is processed into 18S rRNA by cleavage at site D. The 3' product is 27SA2 pre-rRNA, which requires completion of Pol I transcription for its release. In the major pathway, 27SA2 is processed via 27SA3 to 27SB, which is cleaved at site C2 (in ITS2) into 7S and 26S pre-rRNAs – the precursors to the 5.8S and 25S rRNAs.

Figure S2. Over-expression of Rnh201 in *top1Δ* strain does not affect accumulation of pre-rRNA fragments.

WT (BY4741) and *top1Δ* strains were transformed with plasmids *pGAL1* (vector) or *pGAL:RNH201-HA* (see Table S1) and grown in synthetic medium lacking uracil at 25°C in presence of either glucose or galactose to repress or induce, respectively, the expression of Rnh201-HA. **(A)** Total RNA was analyzed by Northern hybridization using probe 130 (upper panel). SCR1 was used as a loading control (lower panel). Intact pre-rRNAs and truncated pre-rRNA fragments are labeled. (18S) and (25S) indicate the position of migration of 18S and 25S rRNAs. Primer names are bracketed (see Fig. 1A for location of primers). **(B)** Western-blot (anti-HA) showing over-expression of Rnh201-HA in the presence of galactose.

Figure S3. Northern analysis of short RNAs (pre-rRNAs, rRNAs, and rRNA fragments) from *TOP1* and *top1Δ* strains.

Total RNA from WT strain (BY4741), mutants *top1Δ*, *rrp6Δ* and *top1Δ rrp6Δ* (same samples as used in Fig. 1), mutants *P_{GAL}-TOP1* and *P_{GAL}-TOP1 rnh1Δ rnh201Δ*, and mutants *P_{GAL}-TOP2* and *P_{GAL}-TOP2 top1Δ* (same samples as in Fig. 3), were resolved on a polyacrylamide/urea gel and analyzed by northern hybridization. The membrane was hybridized successively with probes 130 **(A)**, 003 **(B)**, 020 **(C)**, 017 **(D)** and 041 **(E)**. Intact pre-rRNAs and truncated pre-rRNA fragments are labeled. Heterogeneous truncated pre-rRNA fragments are indicated by stars. Primer names are bracketed (see Fig. 1A for location of primers). Positions of migration of RNA Century Plus ladder (Ambion) are indicated.

Figure S4. Study of pre-rRNA truncation in *top2-4 top1Δ* strains.

WT (W303 α) and *top2-4 top1Δ* strains were transformed with plasmids *pGAL1* (vector), *pGAL:RNH1* or *pGAL:RNH201-HA* (see Table S1) and grown in synthetic medium lacking uracil at 25°C in the presence of galactose. At 0.3 OD₆₀₀ the culture was shifted to 37°C for 3.5 hr. As a control *top2-4 top1Δ* mutant was grown in YPD medium at 25°C then shifted to 37°C for 2 hr. Total RNA was analyzed by northern hybridization. The membrane was successively hybridized with probes 130 (A), 003 (B) and 004 (C). Intact pre-rRNAs and truncated pre-rRNA fragments are labeled. (18S) and (25S) indicate the position of migration of 18S and 25S rRNAs. Probe names are bracketed (see Fig. 1A for location of primers).

Analysis of pre-rRNA truncation in the *top1Δ top2-ts* mutant at 25°C showed increased accumulation of species 1 and 3 relative to species 4, in comparison to single *top1Δ* strains at 25°C (compare Fig. S4A lane 1 with Fig. 2A lane 4). This could be due to a stronger block to transcription elongation in the 5'-region of 18S when the absence of Top1 is combined with impaired Top2 function (*top2-4* allele). After 2 hr at 37°C accumulation of species 3 was greatly reduced in *top1Δ top2-ts* cells (Fig. S4A lane 2), indicative of loss of rRNA transcription in this mutant.

Figure S5. RNA/DNA hybrids obtained by ChIP using S9.6 antibody are digested by RNase H *in vitro*.

RNA/DNA hybrids obtained by immunoprecipitation of crosslinked-and-sheared chromatin from WT cells (BY4741) using S9.6 antibody were treated with RNase H for 2 or 4 hr, high levels of RNases A + T1, DNase I or mock treated, as described in Supplementary Methods. RNA/DNA hybrids were immunoprecipitated a second time with S9.6 antibody. QPCRs were performed using primers **a** (igs2-0), **d** (1-18S2) and **i** (25S3) (see Table S3) and values were normalized to values of primers **a**. Digestion of the RNA strand in RNA/DNA hybrids (R-loops) by RNase A has previously been reported (see p. 2297 in (Thomas et al. 1976)).

Figure S6. EM analysis of long Pol I pileups visualized on rDNA genes from WT and mutants *P_{GAL}-TOP1* and *P_{GAL}-TOP1 rnh1Δ rnh201Δ* after 6 h of Top1 depletion.

(A) Schematic showing the position of the “leading polymerase” in a pile-up of 15 polymerases. The Pol I footprint measured by EM is ~50 bp, so the length of this pile-up is predicted to be ~750 bp (occupying ~2.22 segments of ~337 bp each). The promoter is depicted by an arrow.

(B) Plot is as described in Fig. 6B but including the positions of the leading polymerase in only long pileups (20 or more polymerases) visualized on rDNA genes that could be traced unambiguously from 5' to 3'.

Figure S7. Lack of correlation between the length of polymerase pileups and length of the downstream polymerase-free gap.

The lengths of the polymerase-free gaps downstream of the pileups (i.e., from the downstream edge of the pileup to the next downstream polymerase) were measured for the pileups that were scored in Fig. 6B for WT and mutants $P_{GAL-TOP1}$ and $P_{GAL-TOP1} rnh1\Delta rnh201\Delta$ after 6 hr of Top1 depletion. Shown are scatter plots of the data with linear regression trendlines as derived in Excel.

Table S1. Yeast strains and plasmids used in this study

Strains/Plasmids	Genotype	Reference
<u>Strains:</u>		
BY4741	<i>MATa his3Δ1 leu2Δ0 met15Δ0 ura3Δ0</i>	
YAEH261	BY4741 but <i>top1Δ</i> (HphMx6)	This study
YAEH236	BY4741 but <i>rrp6Δ</i> (NatMx6)	This study
YAEH291	BY4741 but <i>top1Δ</i> (HphMx6) <i>rrp6Δ</i> (NatMx6)	This study
YAEH229	BY4741 but <i>rrp6Δ</i> (NatMx6) <i>trf4Δ</i> (KanMx6)	This study
YAEH230	BY4741 but <i>top1Δ</i> (HphMx6) <i>trf4Δ</i> (NatMx6)	This study
BY4741 but	<i>rnh1Δ</i> (KanMx6)	Euroscarf
BY4741 but	<i>rnh201(35)Δ</i> (KanMx6)	Euroscarf
YAEH241	BY4741 but <i>rnh1Δ</i> (KanMx6) <i>rrp6Δ</i> (NatMx6)	This study
YAEH242	BY4741 but <i>rnh201Δ</i> (KanMx6) <i>rrp6Δ</i> (NatMx6)	This study
YAEH243	BY4741 but <i>rnh1Δ</i> (KanMx6) <i>top1Δ</i> (HphMx6)	This study
YAEH244	BY4741 but <i>rnh201Δ</i> (KanMx6) <i>top1Δ</i> (HphMx6)	This study
YAEH245	BY4741 but <i>top1Δ</i> (HphMx6) <i>rrp6Δ</i> (NatMx6) <i>rnh1Δ</i> (KanMx6)	This study
YAEH246	BY4741 but <i>top1Δ</i> (HphMx6) <i>rrp6Δ</i> (NatMx6) <i>rnh201Δ</i> (KanMx6)	This study
YAEH255	BY4741 but <i>rnh1Δ</i> (KanMx6) <i>rnh201Δ</i> (NatMx6)	This study
YAEH266	BY4741 but + pGAL1	This study
YAEH267	BY4741 but <i>top1Δ</i> (HphMx6) + pGAL1	This study
YAEH268	BY4741 but + pGAL1: <i>RNH201-HA</i>	This study
YAEH269	BY4741 but <i>top1Δ</i> (HphMx6) + pGAL1: <i>RNH201-HA</i>	This study
YAEH271	BY4741 but <i>P_{GAL1}-3HA-TOP1</i> (KanMx6)	This study
YAEH275	BY4741 but <i>P_{GAL1}-3HA-TOP1</i> (KanMx6) <i>rnh201Δ</i> (NatMx6) <i>rnh1Δ</i> (HphMx6)	This study
YAEH278	BY4741 but <i>P_{GAL1}-3HA-TOP2</i> (KanMx6)	This study
YAEH279	BY4741 but <i>P_{GAL1}-3HA-TOP2</i> (KanMx6) <i>top1Δ</i> (HphMx6)	This study
YAEH316	YAEH271 but <i>P_{GAL1}-3HA-TOP2</i> (HIS3)	This study
YAEH317	YAEH275 but <i>P_{GAL1}-3HA-TOP2</i> (HIS3)	This study
YAEH161	BY4741 but <i>RPA34-13MYC</i> (HphMx6)	This study
YAEH252	BY4741 but <i>RPA34-13MYC</i> (HphMx6) <i>top1Δ</i> (KanMx6)	This study
BY4741 but	<i>rpa34Δ</i> (KanMx6)	Euroscarf
BY4741 but	<i>rpa49Δ</i> (KanMx6)	Euroscarf
BY4741 but	<i>hmo1Δ</i> (KanMx6)	Euroscarf
YAEH237	BY4741 but <i>rpa34Δ</i> (KanMx6) <i>rrp6Δ</i> (NatMx6)	This study
YAEH239	BY4741 but <i>rpa49Δ</i> (KanMx6) <i>rrp6Δ</i> (NatMx6)	This study
YAEH238	BY4741 but <i>hmo1Δ</i> (KanMx6) <i>rrp6Δ</i> (NatMx6)	This study
W303α	<i>Matα leu2-3,112 trp1-1 can1-100 ura3-1 ade2-1, his3-11,15</i>	
W1477-5B	W303α but <i>top1::HIS3 top2-4^{ts}</i>	(Rodney Rothstein)
YAEH318	W303α but + pGAL1	This study
YAEH319	W303α but + pGAL1: <i>RNH201-HA</i>	This study
YAEH320	W303α but + pGAL1: <i>RNH1</i>	This study
YAEH321	W1477-5B but + pGAL1	This study
YAEH322	W1477-5B but + pGAL1: <i>RNH201-HA</i>	This study
YAEH323	W1477-5B but + pGAL1: <i>RNH1</i>	This study

Plasmids:

pGAL1 (BG1766) and pGAL1:*RNH201-HA* (Kind gift from Brian Luke, see (Luke et al. 2008))
p416-GAL1 and pGAL1:*RNH1* (Kind gift from Andrés Aguilera, see (Huertas and Aguilera 2003))

Table S2. Oligonucleotides used in Northern hybridizations

Name Oligonucleotide Sequence (5' to 3')

001: CCAGTTACGAAAATTCTTG

020: TGAGAAGGAAATGACGCT

003: TGCTTACCTCTGGGCC

004: CGGTTTTAATTGTCCTA

007: CTCCGCTTATTGATATGC

008: CATGGCTTAATCTTTGAGAC

033: CGCTGCTCACCAATGG

130: ACACGCTGTATAGAGACTAGGC

PGK1: ACCGTTTGGTCTACCCAAGTGAGAAGCCAAGACA

SCR1: ATCCCGGCCGCCTCCATCAC

Primers used for *IGS2* random priming probe (see also (Houseley et al. 2007):

NTS2 F1: GATAGTTTAACGGAAACGCAGGTGA

NTS2 R1: GAAGTACCTCCCAACTACTTTTCCT

Table S3. QPCR primers

Name Oligonucleotide Sequence (5' to 3') Position relative to the transcription start site (+1)

a) igs2-0-F	(CCCTCCCATTACAAACTAAA;	-53),
a) igs2-0-R	(GGCGAGAAATACGTAGTTAAG,	-133),
b) 35S-F	(CCACGATGAGACTG TTCAGG;	+107),
b) 35S-R	(GTCGCTAGGTGATCGTCAGA;	+249),
c) 5-ETS-F	(AACAGCTGAAATTCCAGAAA;	+480),
c) 5-ETS-R	(CTATGGTATGGTGACGGAGT;	+592),
d) 1-18S2-F	(TCCAATTGTTCTCGTTAAG;	+1153),
d) 1-18S2-R	(ATTCAGGGAGGTAGTGACAA;	+1250),
e) 18S-centre-F	(CGATCCCTAGTCGGCATAGT;	+1595),
e) 18S-centre-R	(GAGGTGAAATTCTTGATTTATTG;	+1746),
f) 18S1-F	(GAGGCCTCACTAAGCCATTC;	+2297),
f) 18S1-R	(ATCAGCTTGCGTTGATTACG;	+2377),
g) 5.8S-F	(GCAATGTGCGTTCAAAGATT;	+2894),
g) 5.8S-R	(ATGAAGAACGCAGCGAAAT;	+2976),
h) 25S4-F	(TTCAGCGGGTACTCCTACCT;	+3165),
h) 25S4-R	(ACCAACTGCGGCTAATCTTT;	+3286),
i) 25S3-F	(TTACACCCAAACACTCGCAT;	+3835),
i) 25S3-R	(GACTGAGGACTGCGACGTAA;	+3942),
j) 25S2-F	(GAATCCATATCCAGGTTCCG;	+4765),
j) 25S2-R	(GACGTGGGTTAGTCGATCCT;	+4879),
k) 25S1-F	(ACGCTTACCGAATTCTGCTT;	+6091),
k) 25S1-R	(CGTTCATAGCGACATTGCTT;	+6176),
l) igs1-3-F	(CAGTCTACTTCTCTCTAAACTAGGC;	+6603),
l) igs1-3-R	(TGTTGTTACGATCTGCTGAG;	+6671),
m) igs1-2-F	(ACTCATGTTTGCCGCTCTG;	+6897),
m) igs1-2-R	(TGCAAAGATGGGTTGAAAGA;	+7016),
n) igs1-1-F	(TACACCCTCGTTTAGTTGCTTCT;	+7376),
n) igs1-1-R	(CGGTATGCGGAGTTGTAAGA;	+7478),
o) 5S-F	(ACCTGCGTTTCCGTTAACT;	+7847),
o) 5S-R	(AGTTGATCGGACGGGAAAC;	+7917),
p) igs2-2-F	(GCCACCATCCATTTGTCTTT;	+8125),
p) igs2-2-R	(TGAAAGTTGGTCGGTAGGTG;	+8211)

Supplementary Methods

RNA analysis

Standard 1.2% agarose/glyoxal gel or 8% polyacrylamide/8.3M urea gels were used to resolve high or low molecular weight RNAs, respectively. 5 µg of total RNA were loaded per lane. To detect ncRNAs from IGS1 and IGS2, a random primed probe was prepared using Strip-EZTM (Ambion) (see also (Houseley et al. 2007)).

PolyA RNA extraction using 125 µg Total RNA was done with the 'PolyA Tract mRNA Isolation System IV' and according to the instructions of the supplier (Promega) with some modifications (see also (Dez et al. 2006)). Biotinylated-Oligo (dT)/ Poly A RNA annealing reaction was incubated with Streptavidin Paramagnetic Particles (SA-PMPs) for 1 hour at room temperature using a rotating wheel. SA-PMPs were then washed 5 times with 0.2X SSC and PolyA RNAs were finally eluted from the beads at 65°C with water.

Northern membranes were imaged using a Fuji FLA-5100 and RNA bands in Fig. 4 were quantified using Aida software (Raytest).

ChIPs

Crosslinking with formaldehyde (1%) was for 25 min. Protein A sepharose beads (GE Healthcare) were used with S9.6 and anti-Rpa190, and Gammabind Plus beads (GE Healthcare) for anti-MYC. EXPRESS SYBR® GreenER(tm) qPCR Supermix Universal (Invitrogen) was used for Q-PCR reactions.

EM analyses

In Figs. **6** and **S6**, WT, $P_{GAL-TOP1}$ and $P_{GAL-TOP1} rnh1\Delta rnh201\Delta$ strains grown in YP-Gal were shifted to YPD for 6 hr prior to chromatin spreading. The experiment was done twice and all nucleoli visualized by EM were photographed. Ribosomal RNA genes that could be unambiguously traced as individual genes were analyzed for number of polymerases and occurrence of polymerase pileups (5 or more very closely positioned polymerases). Excluded from the analyses (in Figs. **6B**, **D**, **E** and **S6**) were 6% of genes from $P_{GAL-TOP1}$ and 0.4% of genes from $P_{GAL-TOP1} rnh1\Delta rnh201\Delta$ strains. These genes exhibited DNA template opening due to negative topological stress and are included in another study (French et al. submitted).

Their exclusion did not significantly change the quantitative parameters studied herein. Gene lengths were normalized for mapping pileup positions.

In Fig. **6C**, polymerase occupancy was measured along 77 rDNA genes that were being actively transcribed from 5' to 3' end, for each of the 3 strains (WT, *P_{GAL}-TOP1* and *P_{GAL}-TOP1 rnh1Δ rnh201Δ*). For the WT strain, all analyzable genes whose 5' and 3' ends could be accurately determined were included, giving a total of 77. For the two mutants, genes were randomly chosen for analysis until a total of 77 was reached, which represented most of the analyzable genes in the datasets in both cases. For accurate mapping of Pol I positions on rDNA genes, it was important to determine the positions of both ends of the gene. For this reason, genes whose 5' or 3' ends were largely devoid of polymerases were not included in the analysis. There are no visual cues to locate the ends of the gene in the absence of polymerases, and gene length can vary considerably due to differential stretching of the DNA in chromatin spreads. In an initial crude analysis of 518 genes from the 3 strains, 57 genes were scored as having a 5' and/or 3' end that was difficult to map due to lack of polymerases, indicating that ~11% of active genes were excluded for this reason.

In Fig. **S7**, pile-up and gap lengths were measured from polymerase centre to polymerase centre. For gaps, the distance between the upstream (3') and downstream (5') polymerase should effectively be one polymerase-width less (or - ~50nt) than measured. For pile-ups, the distance between the 3' and 5' ends should effectively be one polymerase-width more (or + ~50nt).

Sequential Analysis of RNA/DNA hybrids: ChIP-digestion with nuclease-DIP

A. ChIP

Wild-type yeast cells (BY4741) were grown in YPD medium at 30°C to 0.7 A₆₀₀/ml and crosslinked for 5 min with formaldehyde 1%. ChIP with S9.6 antibody was performed as described in Material and Methods and (El Hage et al. 2008). Following reversal of the crosslink and deproteinization, DNA samples were purified with Qiagen PCR purification kit and eluted with water. DNA was then subsequently treated with nucleases (**B**) and immunoprecipitated with S9.6 antibody (**C**) as described below.

B. Digestion with nucleases

RNase H: DNA (1.68 μg) from step A was adjusted with NEB 10X RNase H buffer to final concentrations of 75 mM KCl, 50 mM Tris-HCl pH 8.3, 3 mM MgCl₂ and 10 mM DTT. Glycerol and BSA were added to final concentrations of 4% and 20 μg ml⁻¹, respectively (as described in (Nowotny et al. 2005)). DNA was incubated at 37°C in the absence (for 2hr) or presence (for 2, 4

or 6 hr) of 50 u of RNase H (NEB). EDTA was added to final concentration 10 mM to stop the reaction.

RNases A/T1: DNA (1.68 µg) from step A was adjusted to final concentrations of 75 mM KCl and 50 mM Tris-HCl pH 8.3. DNA was incubated for 2 hr at 37°C in the presence of 15 u of RNase A plus 600 u of RNase T1 (RNase Cocktail Enzyme Mix, Ambion). EDTA was added to final concentration 10 mM at the end of the incubation. Note that at low salt concentrations (e.g. 0 to 100 mM NaCl), RNase A cleaves single-stranded and double stranded RNA as well the RNA strand in RNA-DNA hybrids (see (Nichols and Yue 2008) and

http://www.fermentas.com/templates/files/tiny_mce/coa_pdf/coa_en0531.pdf)

DNase I: DNA (1.68 µg) from step A was adjusted with 10x RQ1 DNase I buffer (Promega) to final concentrations of 40 mM Tris-HCl pH 8, 100 mM MgSO₄ and 100 mM CaCl₂. DNA was incubated for 1 hr at 37°C in the presence of 6 u of RQ1 RNase-free DNase I (Promega). EDTA was added to final concentration 20 mM to stop the reaction.

C. DIP (DNA immunoprecipitation)

DIP using S9.6 antibody was done mainly as described for CHIP (see (El Hage et al. 2008)) but with some exceptions. Control and RNase H-treated samples from **B** were diluted 10 times with a buffer containing 100 mM KCl, 50 mM Tris- HCl pH 8 and 10 mM EDTA, in order to decrease the concentration of DTT to 1mM. Triton X-100 and sodium deoxycholate were added to all samples from **B** to final concentrations of 1% and 0.1% (w/v), respectively. Each sample (1.68 µg of DNA) from **B** was split in 2 equal parts: one served as no-antibody control and the other one for DIP with S9.6 antibody. Gammabind Plus sepharose beads (GE Healthcare) were used for immunoprecipitation. CPI 1x (Roche Complete Protease Inhibitor) was omitted. Washings of beads were performed subsequently with a buffer containing 75 mM KCl, 50 mM Tris-HCl pH 8, 1% Triton X-100 and 0.1% (w/v) sodium deoxycholate (3x10 min), with the same buffer but supplemented with 300 mM KCl (1x20min), and finally with TE buffer containing 10 mM Tris-HCl pH 8 and 1 mM EDTA pH 8 (2x15min).

Western Blots

Total proteins extracts and western blot analysis were performed using standard procedures. Rnh201-HA was detected with mouse anti-HA sc-7392 antibody (Santa Cruz Biotechnology).

SUPPLEMENTARY REFERENCES

- Dez, C., Houseley, J., and Tollervey, D. 2006. Surveillance of nuclear-restricted pre-ribosomes within a subnucleolar region of *Saccharomyces cerevisiae*. *Embo J* **25**(7): 1534-1546.
- El Hage, A., Koper, M., Kufel, J., and Tollervey, D. 2008. Efficient termination of transcription by RNA polymerase I requires the 5' exonuclease Rat1 in yeast. *Genes Dev* **22**(8): 1069-1081.
- French, S.L., Sikes, M.L., Hontz, R.D., Osheim, Y.N., Lambert, T.E., Hage, A.E., Smith, M.M., Tollervey, D., Smith, J.S., and Beyer, A.L. submitted. Distinguishing the roles of Topoisomerase I and II in relief of transcription-induced torsional stress in yeast rDNA genes.
- Houseley, J., Kotovic, K., El Hage, A., and Tollervey, D. 2007. Trf4 targets ncRNAs from telomeric and rDNA spacer regions and functions in rDNA copy number control. *Embo J* **26**(24): 4996-5006.
- Huertas, P. and Aguilera, A. 2003. Cotranscriptionally formed DNA:RNA hybrids mediate transcription elongation impairment and transcription-associated recombination. *Mol Cell* **12**(3): 711-721.
- Kos, M. and Tollervey, D. 2010. Yeast Pre-rRNA Processing and Modification Occur Cotranscriptionally. *Mol Cell* **37**(6): 809-820.
- Luke, B., Panza, A., Redon, S., Iglesias, N., Li, Z., and Lingner, J. 2008. The Rat1p 5' to 3' Exonuclease Degrades Telomeric Repeat-Containing RNA and Promotes Telomere Elongation in *Saccharomyces cerevisiae*. *Mol Cell* **32**(4): 465-477.
- Nichols, N. and Yue, D. 2008. in *Current Protocols in Molecular Biology*, pp. 3.13.11-13.13.18. Wiley Interscience (www.interscience.wiley.com).
- Nowotny, M., Gaidamakov, S.A., Crouch, R.J., and Yang, W. 2005. Crystal structures of RNase H bound to an RNA/DNA hybrid: substrate specificity and metal-dependent catalysis. *Cell* **121**(7): 1005-1016.
- Osheim, Y.N., French, S.L., Keck, K.M., Champion, E.A., Spasov, K., Dragon, F., Baserga, S.J., and Beyer, A.L. 2004. Pre-18S ribosomal RNA is structurally compacted into the SSU processome prior to being cleaved from nascent transcripts in *Saccharomyces cerevisiae*. *Mol Cell* **16**(6): 943-954.
- Thomas, M., White, R.L., and Davis, R.W. 1976. Hybridization of RNA to double-stranded DNA: formation of R-loops. *Proc Natl Acad Sci U S A* **73**(7): 2294-2298.
- Warner, J.R. and Kim, H.S. 2010. The Fast Track Is Cotranscriptional. *Mol Cell* **37**(6): 745-746.

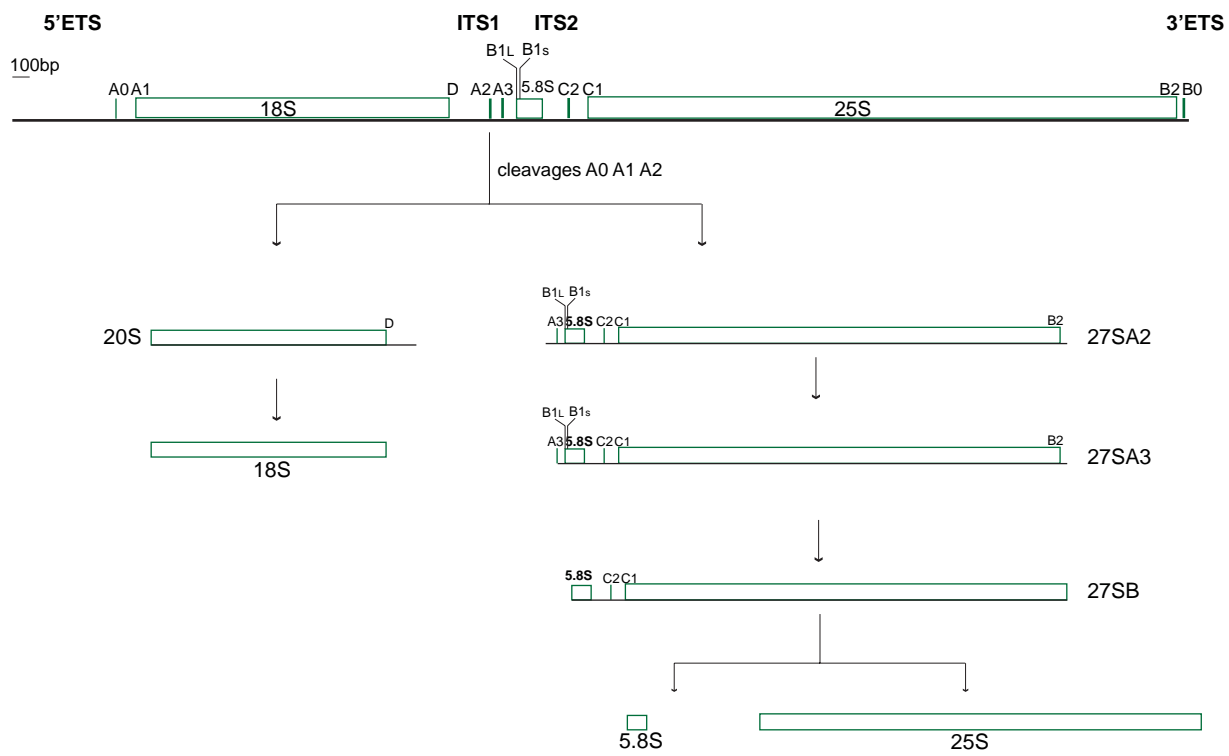


Fig.S1

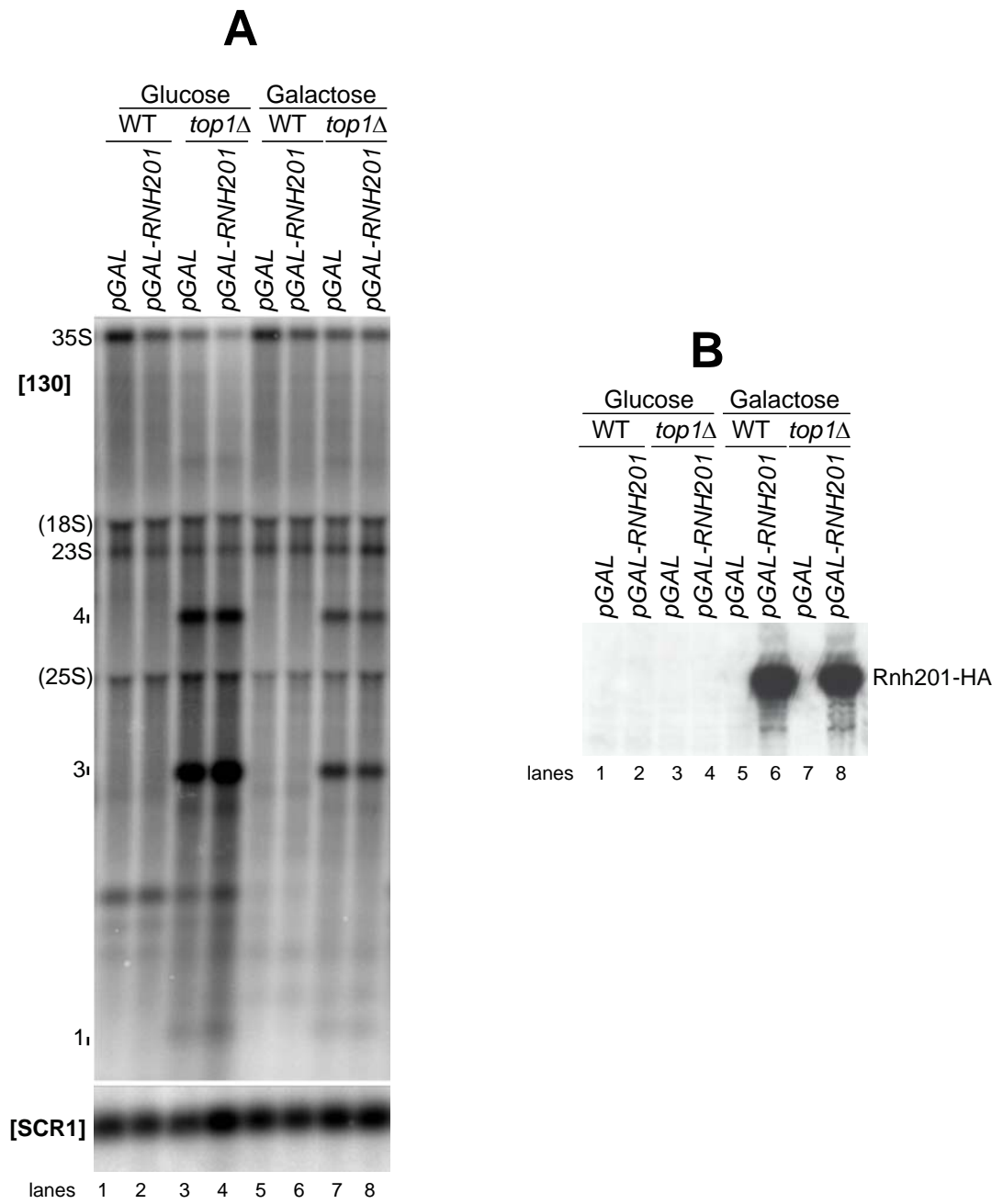


Fig.S2

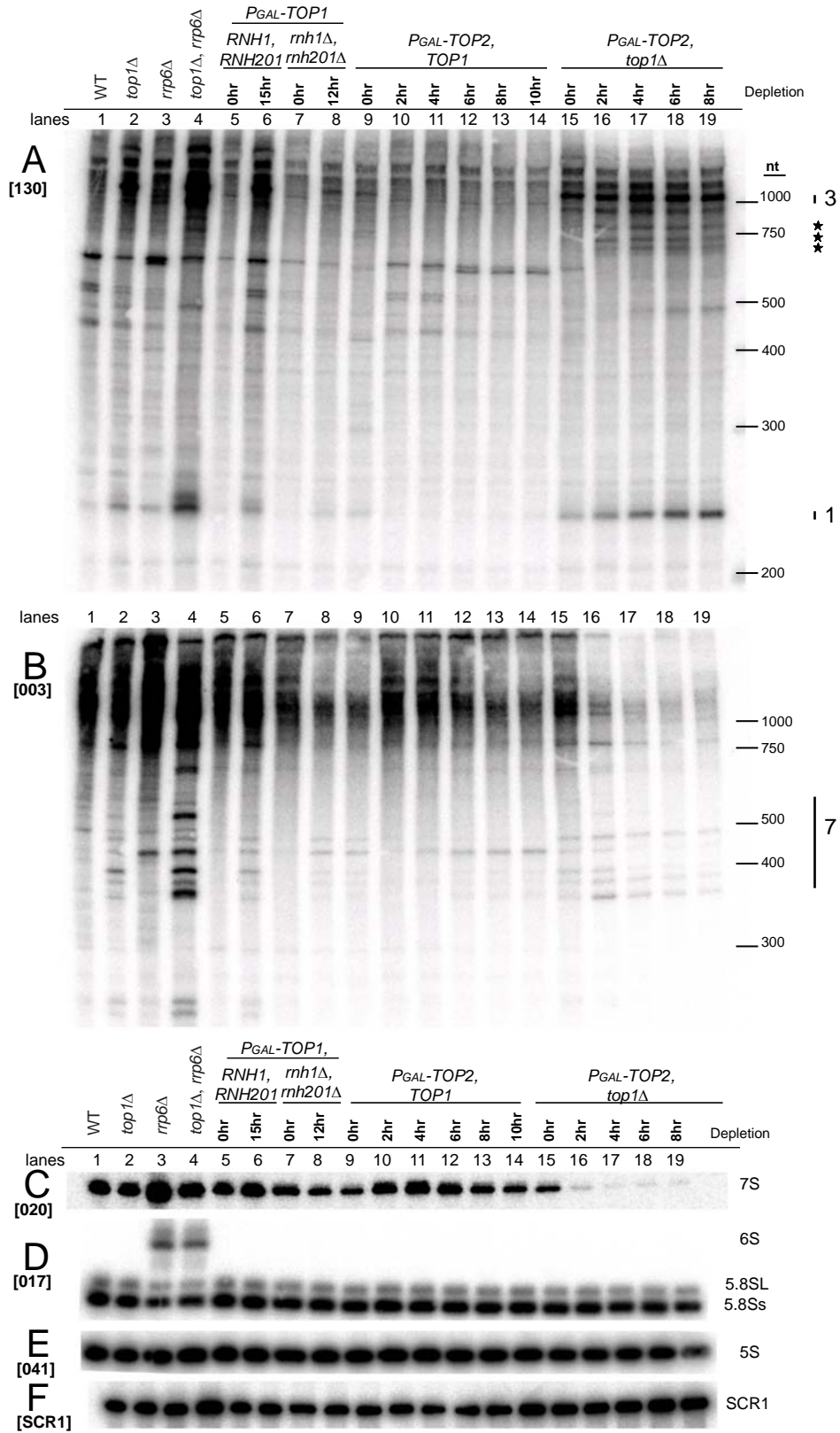


Fig.S3

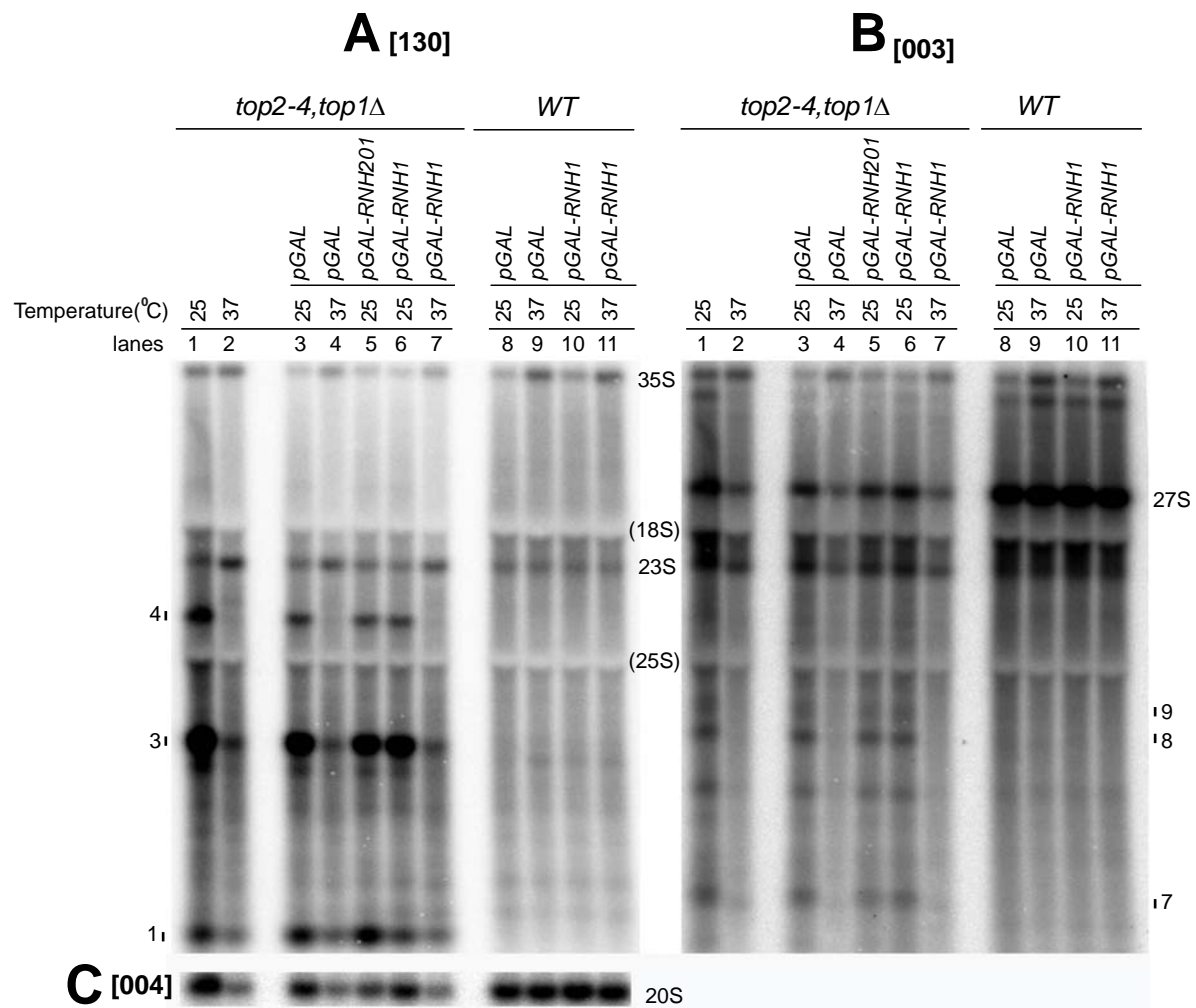


Fig.S4

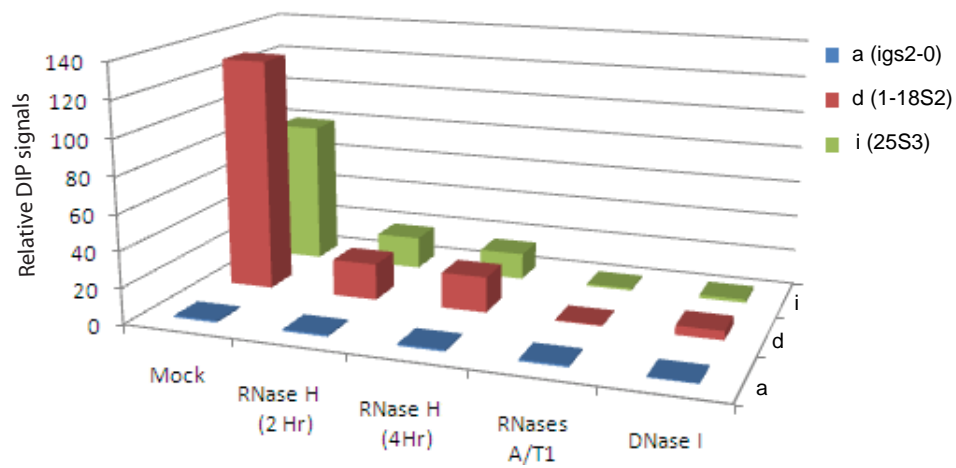


Fig.S5

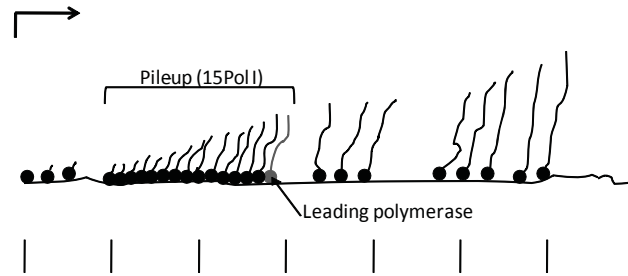
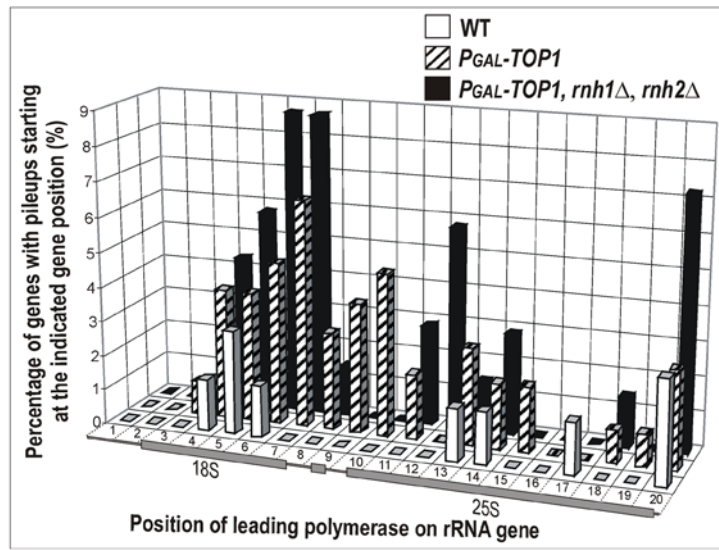
A**B**

Fig.S6

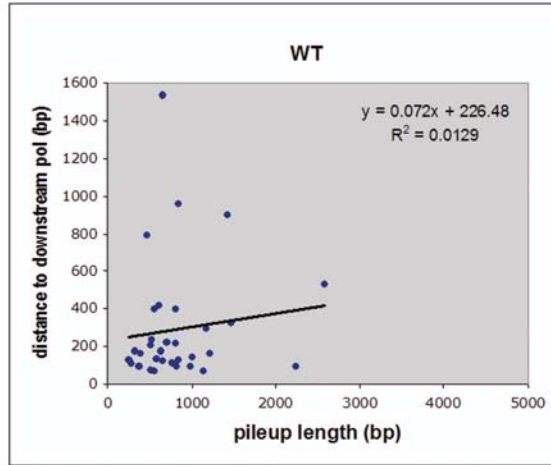
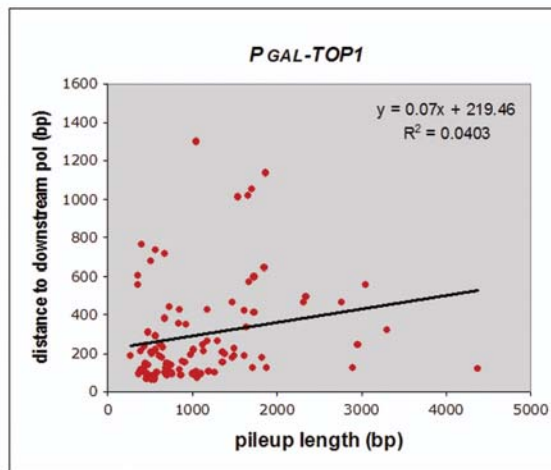
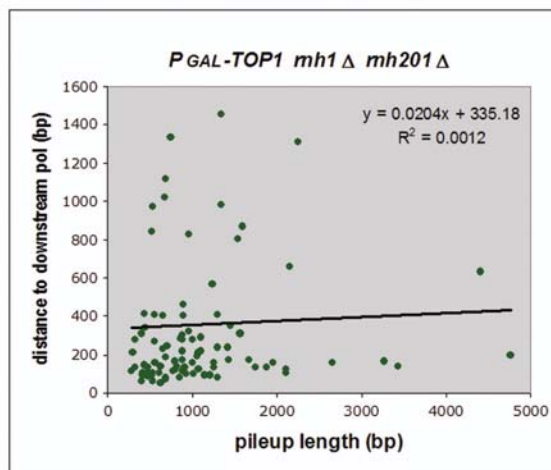
A**B****C**

Fig.S7